THE UNIVERSITY OF MICHIGAN
INDUSTRY PROGRAM OF THE COLLEGE OF ENGINEERING

A SIMPLE MODEL STUDY OF TRANSIENT TEMPERATURE AND THERMAL STRESS DISTRIBUTION DUE TO AERODYNAMIC HEATING

Gabriel Isakson

July, 1956

IP-169

ACKNOWLEDGEMENT

We wish to express our appreciation to the author for permission to give this paper limited distribution under the Industry Program of the College of Engineering.

PREFACE

This paper represents a condensation of portions of a thesis[10] submitted by the author to the Massachusetts Institute of Technology in March, 1953, in partial fulfillment of the requirements for the degree of Doctor of Science. The work was carried out in connection with U. S. Air Force Contract AF33(616)-3259 in the Aero-elastic and Structures Research Laboratory at the Massachusetts Institute of Technology under the direction of Professor R. L. Bisplinghoff. The author is especially indebted to Mr. C. W. Brenner for assistance with the Whirlwind I digital computations and Mr. W. Campbell for assistance in the experimental phases of the work. Availability of time on the Whirlwind I digital computer was made possible by the Office of Naval Research. The preparation of this paper was aided materially by the Industry Program of the College of Engineering of the University of Michigan.

TABLE OF CONTENTS

LIST OF FIGURES

LIST OF FIGURES (CONT.)

LIST OF FIGURES (CONT.)

ABSTRACT

The present work is concerned with the determination of transient temperatures and thermal stresses in simple models intended to simulate parts or the whole of an aircraft structure of the built-up variety subjected to aerodynamic heating.

The first case considered is that of convective heat transfer into one side of a flat plate, representing a thick skin, and the effect of the resulting temperature distribution in inducing thermal stresses associated with bending restraint at the plate edges. Numerical results are presented for the transient temperature distribution in the plate when the environment temperature first increases linearly with time and then remains constant, the period of linear increase representing the time of acceleration of the aircraft. The results indicate that this time must be considerable if substantial reduction of temperature differentials is to be effected. Corresponding thermal stress information is presented. Temperature differentials and thermal stresses are presented as functions of the Mach number of the external flow for various materials and skin thicknesses, and comparisons are made for the purpose of evaluating the suitability of these materials.

The second case is that of the wide-flanged I-beam with convective heat transfer into the outer faces of the flanges. Numerical results are presented for the transient temperature distribution for a wide range of values of the applicable parameters and for an environment temperature variation as described above. Corresponding thermal stresses in a beam of infinite length are determined. A theoretical analysis of the stress distribution in a beam of finite length is carried out and numerical results obtained for one case. An experimental investigation of temperatures and stresses in such a beam is described, and results are presented which indicate good agreement with corresponding theoretical results.

LIST OF SYMBOLS

b = semi-width of I-beam

c_p = specific heat of plate or beam material

$f(\xi)$ = non-dimensional temperature distribution in plate, $\frac{T - T_{x=0}}{\Delta T}$

h = heat transfer coefficient at heated surface

h_j = heat transfer coefficient at joint between beam flange and web

k = thermal conductivity of plate or beam material

ℓ = semi-length of I-beam

s = semi-depth of I-beam

t = time

t_g = time of linear increase of environment temperature

u = displacement in x-direction

x = coordinate in plate representing distance from insulated surface, positive toward heated surface

x,y,z = coordinates of I-beam (Figures 13 and 20)

A_f, A_w = cross-sectional area of flanges and web respectively of I-beam

A_{mn} = coefficients in series for Airy stress function for flange

B_{mn} = coefficients in series for Airy stress function for web

E = Young's modulus of elasticity

M = Mach number

$SCFC$ = stress correction factor for compression (Eq. 15)

$SCFT$ = stress correction factor for tension (Eq. 16)

$(SCFC)_m$ = modified stress correction factor for compression (Eq. 17)

$(SCFT)_m$ = modified stress correction factor for tension (Eq. 18)

T = temperature in plate or beam

T_o = temperature at middle of beam web

ΔT = temperature differential between surfaces of plate, temperature differential between middle of web and edge of flange

T_i = initial temperature in plate or beam

T_e = environment temperature

T_{e_r} = reference environment temperature

V = strain energy

α = coefficient of thermal expansion

γ = ratio of flange thickness to web thickness, δ_f / δ_w

δ = plate thickness

ζ = non-dimensional beam coordinate, z/ℓ

η = non-dimensional beam coordinate, y/s

κ = thermal diffusivity of plate or beam material, $\frac{k}{\rho c_p}$

λ = non-dimensional heating parameter, $\frac{h\delta}{k}$ in plate, $\frac{hs^2}{k\delta_f}$ in I-beam

λ_j = non-dimensional heat transfer coefficient at web-flange joint, $h_j s/k$

μ = $2 + \nu$

ν = Poisson's ratio

ξ = non-dimensional beam coordinate, x/δ in plate, x/s in I-beam in Section IV, x/b in I-beam in Sections V and VI

ρ = density of plate or beam material

$\sigma_x, \sigma_y, \sigma_z$ = normal stress components

σ_n = intensity of normal force applied on edge of plate

σ_o = intensity of normal force applied on end of beam

τ = non-dimensional time variable, $\frac{\kappa t}{\delta^2}$ in plate, $\frac{\kappa t}{s^2}$ in beam

τ_g = non-dimensional time of linear increase of environment temperature

LIST OF SYMBOLS (Cont.)

$(\tau_g)_r$ = $\dfrac{\tau_g}{\tau \text{ at } (\Delta\phi)_{max.}\ \tau_g=0}$

$\tau_{xy}, \tau_{yz}, \tau_{xz}$ = shear stress components

ϕ = non-dimensional temperature, $\dfrac{T_{e_r}-T}{T_{e_r}-T_i}$, Airy stress function

ϕ_e = non-dimensional environment temperature, $\dfrac{T_{e_r}-T_e}{T_{e_r}-T_i}$

$\Delta\phi$ = $\dfrac{\Delta T}{T_{e_r}-T_i}$

ψ = ratio of I-beam length to width, ℓ/b

ω = ratio of I-beam width to depth, b/s

Subscripts:

f = flange

w = web

I. INTRODUCTION

In the rapid acceleration of an aircraft to very high speed, friction in the boundary layer may raise the temperature of the surface of the aircraft with sufficient rapidity that large temperature differentials may occur in the structure before interior portions heat up. This may result in thermal stresses of considerable magnitude.

The heat transfer into the surface of the aircraft may be treated in a manner similar to convective heat transfer in low speed flow. An appropriate heat transfer coefficient is used in conjunction with the difference between the temperature at the solid surface and the so-called "adiabatic wall temperature", or temperature which would be attained in the air at the solid surface if that surface were insulated.[1] The heat transfer coefficient and adiabatic wall temperature depend upon the properties of the ambient air, the velocity of flow outside the boundary layer, and the thickness and type of boundary layer (laminar or turbulent).

Determination of the transient temperature and thermal stress distribution in the case of a typical built-up aircraft structure is exceedingly difficult and cumbersome. Much of a general nature can be learned, however, from the analysis of simple structures representing parts of the built-up structure or constituting simple models intended to represent the whole structure.

Thus, in the present work, attention is concentrated on the flat plate with convective heat transfer into one face and the wide-flanged I-beam with convective heat transfer into the outer faces of the flanges. The former is intended to represent the thick skin of a high-speed aircraft, while the latter is intended to represent a simple type of built-up wing structure. The interior surfaces of the structure are assumed to be insulated. Heat transfer by radiation or convection between parts of the structure is neglected.

II. TRANSIENT TEMPERATURE DISTRIBUTION IN A FLAT PLATE

The case of a flat plate insulated on one side and with convective heat transfer on the other side is first considered. The following assumptions are made.

(1) The environment temperature and heat transfer coefficient are uniform over the heated surface, the latter being constant with time.

(2) The temperature in the plate is initially uniform.

(3) There is no heat transfer through the edges of the plate, so that the flow of heat takes place only in a direction normal to the surface of the plate.

(4) Variation of the thermal properties of the material of the plate with temperature may be neglected.

The partial differential equation for the temperature in the plate is

$$\frac{\partial T}{\partial t} = \kappa \frac{\partial^2 T}{\partial x^2} \tag{1}$$

and the boundary conditions are

(1) At $x = 0$, $\quad \frac{\partial T}{\partial x} = 0$

(2) At $x = \delta$, $\quad \kappa \frac{\partial T}{\partial x} = h(T_e - T)$

(3) At $t = 0$, $\quad T = T_i$

Equation (1) and the boundary conditions may be written in non-dimensional form as follows:

$$\frac{\partial \phi}{\partial \tau} = \frac{\partial^2 \phi}{\partial \xi^2} \tag{2}$$

(1) At $\xi = 0$, $\quad \frac{\partial \phi}{\partial \xi} = 0$

(2) At $\xi = 1$, $\quad \frac{\partial \phi}{\partial \xi} = \lambda(\phi_e - \phi)$

(3) At $\tau = 0$, $\quad \phi = 1$

An equivalent problem for the special case of constant T_e is a familiar one in the field of heat transfer, and its solution is well-known. It is the problem of an infinite plate at initial uniform temperature T_i, subjected suddenly to an environment at constant temperature T_e on both sides. Heat flows into the surfaces of the plate by convective heat transfer.

This problem is seen to be identical with the present problem if, in the former, only half the thickness of the plate is considered, since, because of symmetry, there is no heat flow across the middle surface, which may thus be considered as an insulated surface.

The classical solution to this problem is given as an infinite transcendental series.[2] Numerous charts and tables presenting results for various values of the parameter λ are available in the literature (reference 2, pages 274, 285, 415, 416, and reference 3, page 122). These results are used here to plot a curve of $(\Delta\phi)_{max.}$, that is, the non-dimensionalized maximum temperature differential across the two faces of the plate during the heating period, versus the parameter λ. The non-dimensional time τ at which this

maximum occurs has also been plotted. These plots are shown in Figure 1. It will be shown in the next section that this maximum temperature differential provides a measure of the maximum thermal stress in the plate.

The assumption of constant T_e and h is not realistic for the case of aerodynamic heating, since it implies an infinite acceleration, that is, an instantaneous achievement of high speed flight. In reality, the period of acceleration may be of the order of several minutes, during which time the adiabatic wall temperature, represented here by the environment temperature, and the heat transfer coefficient are increasing. The introduction of a variable heat transfer coefficient would complicate the problem very greatly, however. On the other hand, the introduction of a variable environment temperature does not complicate the problem unduly if its variation is assumed to be of a simple form.

Because of the linearity of the governing differential equation, such a variation of T_e may be taken into account by the application of Duhamel's integral in conjunction with the time history of temperature in the plate following a sudden change in environment temperature.[4]

While the problem may be handled analytically in this manner, it was decided, after considerable investigation, that the use of a finite difference numerical method in conjunction with an automatic digital computing machine would be more expeditious in the generation of a large volume of data. Consequently, a finite difference procedure was set up, as outlined in Appendix A.

The time history of T_e was assumed to have the form shown in Figure 2(a) and represented mathematically as follows:

$$\begin{aligned} T_e &= T_i + (T_{er} - T_i)\frac{t}{t_g} && \text{for} \quad 0 \le t \le t_g \\ &= T_{er} && \text{for} \quad t > t_g \end{aligned} \tag{3}$$

In non-dimensional form, Equation (3) becomes

$$\phi_e = 1 - \frac{\tau}{\tau_g} \qquad \text{for} \quad 0 \le \tau \le \tau_g$$
$$= 0 \qquad \text{for} \quad \tau > \tau_g \tag{4}$$

and is shown in Figure 2(b).

A program of computations was carried out on the Whirlwind I automatic digital computer at the Massachusetts Institute of Technology for a variety of values of the parameters λ and τ_g . The effect of these parameters on the maximum temperature differential attained in the plate is shown in Figure 3.

In addition to the maximum temperature differential, it is also important, for the purpose of thermal stress determination, to know the distribution of temperature through the thickness of the plate. This distribution may be expressed conveniently in terms of the non-dimensional function,

$$f(\xi) = \frac{T - T_{x=0}}{\Delta T} \tag{5}$$

The computed results indicate that, at the time of maximum temperature differential, the function $f(\xi)$ approaches the parabolic form, $f(\xi) = \xi^2$, for low values of λ when T_e varies as a step-function, and for all values of λ when T_e has an initial linear gradient and the non-dimensional gradient time τ_g is sufficiently large. It is thus convenient to adopt this parabolic distribution as a reference distribution. At large values of λ and zero or small values of τ_g , the temperature gradient at the heated surface is more pronounced than that given by the parabolic distribution.

As an illustration of how the temperature distribution changes with time in a particular case, Figure 4 shows the function $f(\xi)$ plotted for a

number of values of τ for the case, $\lambda = 20$ and T_e in the form of a step-function. The curve $f(\xi) = \xi^2$ is included as a reference. It is seen that for this case the parabolic distribution is not obtained until some time after the peak temperature differential has been reached.

The effect of τ_g on the temperature distribution at the instant when the temperature differential, ΔT, is a maximum is shown in Figure 5, again for $\lambda = 20$. It is seen how an increase in τ_g tends to bring the temperature distribution closer to the parabolic form.

Application to the Problem of Aerodynamic Heating.

The information presented in Figure 1 has been applied to the problem of aerodynamic heating to provide data on temperature differentials in structural plating of different thicknesses, for a variety of aircraft structural materials, and for a selected flight condition. The particular alloy chosen in each case is the one which appeared to have desirable properties for use at elevated temperatures.

The thermal conductivity and specific heat of each material were assumed constant, although they are in fact variable with temperature. An attempt was made, wherever possible, to select values corresponding to an average temperature in the range of interest.

The flight condition assumed is that of take-off at sea level, followed by instantaneous achievement of high-speed flight at 50,000 feet altitude. It is, of course, unrealistic, but should provide a satisfactory approximation when the acceleration period is short.

Figure 6 provides information on the maximum temperature differential attained in the plates and the time at which it occurs. These results are presented as a function of flight Mach number for various values of plate thickness.

Where the acceleration period is expected to have a significant alleviating effect, the data of Figure 6 may be modified by using Figure 3 in conjunction with Figure 7 to yield an approximate result within the limitations of the assumptions made in determining Figure 3.

III. THERMAL STRESSES IN A FLAT PLATE

The thermal stresses resulting from transient temperature distributions in a flat plate, as discussed in the preceding section, are now considered.

The usual assumption in plate theory, namely, that stresses in planes normal to the plate may be neglected, is made here. Thus,

$$\sigma_x = \tau_{xy} = \tau_{xz} = 0$$

It is assumed, in addition, that deflections of the plate normal to its plane are small in comparison with its thickness.

From the theory of elasticity it is easily shown that the stress distribution corresponding to zero strain in planes parallel to the surface of the plate is given by

$$\sigma_y = \sigma_z = -\frac{\alpha E (T - T_i)}{1 - \nu} \tag{6}$$

$$\tau_{yz} = 0 \tag{7}$$

This condition requires that a distributed tensile force of intensity,

$$\sigma_n = -\frac{\alpha E (T - T_i)}{1 - \nu} \tag{8}$$

be applied at the edges of the plate, and is obtained when the edges are completely restrained against displacement in planes parallel to the surfaces of the plate.

For other boundary conditions it is necessary to superpose on the stresses of Equations (6) and (7) the stress distribution given by additional

boundary forces necessary to satisfy the boundary conditions. In the case of a plate which is free to stretch or contract in its middle surface, but which is restrained against rotation at its edges, the additional boundary force distribution, $\Delta\sigma_n$, must satisfy the conditions,

$$\int_0^\delta (\sigma_n + \Delta\sigma_n)\, dx = 0 \tag{9}$$

$$\int_0^\delta (x - \tfrac{\delta}{2})\, \Delta\sigma_n\, dx = 0 \tag{10}$$

These conditions are not sufficient to establish the distribution, $\Delta\sigma_n$, more detailed information concerning the manner in which the edge restraint is applied being required. However, the various possible distributions will differ from one another by incremental distributions which are self-equilibrating and which, according to the principle of Saint-Venant, would be effective in stressing the plate only near its edges.

Since the concern here is not with local edge effects, it is permissible to select the simplest possible distribution which will satisfy Equations (9) and (10). This distribution is the uniform distribution given by

$$\Delta\sigma_n = -\frac{1}{\delta}\int_0^\delta \sigma_n\, dx = -\int_0^1 \sigma_n\, d\xi \tag{11}$$

The resulting stress in the plate, except near the edges, is thus given by

$$\sigma_y = \sigma_z = \sigma_n - \int_0^1 \sigma_n\, d\xi \tag{12}$$

and its distribution for a typical temperature distribution is shown in Figure 8.

The plate remains flat in this case, since the bending moment applied at the edges is uniformly transmitted through the plate and eliminates all curvature resulting from thermal expansion. The presence of lateral support in addition to bending restraint at the edges will consequently not alter the result.

With the assumption that α and E do not vary with temperature, and upon substitution of Equations (5) and (8), Equation (12) becomes,

$$\sigma_y = \sigma_z = -\frac{\alpha E \Delta T}{1-\nu} \left\{ f(\xi) - \int_0^1 f(\xi)\, d\xi \right\} \tag{13}$$

For a linear temperature distribution, Equation (13) becomes,

$$\sigma_y = \sigma_z = -\frac{\alpha E \Delta T}{1-\nu} \left(\xi - \tfrac{1}{2}\right) \tag{14}$$

giving a compressive stress $\frac{\alpha E \Delta T}{2(1-\nu)}$ at the heated surface and an equal tensile stress at the insulated surface.

Such a temperature distribution is not consistent with the boundary condition for heat flow at the insulated surface and, as seen in the preceding section, the actual temperature distribution for the type of heating considered will be approximately parabolic in most cases. It is, however, convenient to use the linear distribution for the purpose of computing a reference thermal stress to which a correction factor may then be applied for other temperature distributions. Thus, stress correction factors for compression and tension, respectively, are defined as follows.

$$SCFC = 2\left\{1 - \int_0^1 f(\xi)\, d\xi\right\} \tag{15}$$

$$SCFT = 2\int_0^1 f(\xi)\, d\xi = 2 - SCFC \tag{16}$$

For a parabolic distribution of temperature $(f(\xi) = \xi^2)$,

$$SCFC = \frac{4}{3}$$

$$SCFT = \frac{2}{3}$$

When the temperature gradient at the heated surface is still more pronounced, SCFC will be larger, with 2 as its limiting value, while SCFT will reduce toward zero.

The transient temperature data obtained from the digital computation program have been used to obtain transient stress data. Figure 9 shows the variation of SCFC and SCFT with time for a typical case. Because of this variation, the maximum stresses in the plate are not reached simultaneously with the maximum temperature differential.

In order to express the maximum stresses in terms of the maximum temperature differential, it is desirable to define modified stress correction factors as follows,

$$(SCFC)_m = \frac{\Delta\phi}{(\Delta\phi)_{max.}} \times SCFC \qquad (17)$$

$$(SCFT)_m = \frac{\Delta\phi}{(\Delta\phi)_{max.}} \times SCFT \qquad (18)$$

The maximum values of these modified factors, when multiplied by the maximum temperature differentials, will give the maximum stresses. Their variation with time is shown in Figure 9. It is seen that the maximum compressive stress is reached somewhat earlier and the maximum tensile stress somewhat later than the

maximum temperature differential. The maximum value of $(SCFC)_m$ is 1.55, and consequently considerably greater than the value (1.333) of $SCFC$ for a parabolic temperature distribution. On the other hand, the maximum value of $(SCFT)_m$ is .64 and consequently only slightly less than the value (.667) of $SCFT$ for a parabolic distribution.

In general, for large values of the parameter λ and $\tau_g = 0$, the maximum value of $(SCFC)_m$ tends to be substantially larger than the value of $SCFC$ for a parabolic temperature distribution, while the maximum value of $(SCFT)_m$ tends to be slightly less than the value of $SCFT$ for a parabolic temperature distribution. As λ decreases, the times at which $(SCFC)_m$ and $(SCFT)_m$ reach their peak values approach the time for $(\Delta\phi)_{max.}$, and the peak values of these correction factors approach the corresponding values for a parabolic temperature distribution, namely, 1.333 and .667 respectively. These results are shown for compressive stress in Figure 10 along with the variation of $SCFC$ at $(\Delta\phi)_{max.}$ with λ. In the case of tensile stress, the maximum value of $(SCFT)_m$ is either equal to or slightly less than .667 throughout the range considered, and may thus be taken as .667 in any practical computation.

The effect of τ_g on the value of $SCFC$ at $(\Delta\phi)_{max.}$ is shown in Figure 11. It is seen that $SCFC$ at $(\Delta\phi)_{max.}$ approaches the value 1.333 as τ_g increases. The effect of τ_g on the maximum value of $(SCFC)_m$ was not obtained. It is reasonable to expect, however, that this quantity will approach the value 1.333 as τ_g increases. The maximum value of $(SCFT)_m$ can be expected, in all cases, to remain close to the value .667.

Application to the Problem of Aerodynamic Heating.

The temperature data of Figure 6 have been used to determine thermal stresses for the four materials considered. These stresses were computed on the basis of a linear distribution of temperature through the plate. In order to determine the actual maximum tensile or compressive stress in a particular case, it is thus necessary to apply a stress correction factor, as discussed previously. For this purpose, the appropriate value of λ may be determined from Figure 7. Corrections may also be applied for finite values of γ_g .

The values of E and α were assumed to remain constant with temperature variation in the case of each of the materials. The thermal stress data obtained are presented in Figure 12. In order to indicate how these stresses relate to the strength of the material, they have been divided by the yield strength of the material at the applicable adiabatic wall temperature. As a means of illustrating the relative merits of the various materials, the actual plate thickness has been replaced by an "equivalent thickness" equal to the thickness of an aluminum alloy plate weighing the same as the given plate.

IV. TRANSIENT TEMPERATURE DISTRIBUTION IN A WIDE-FLANGED I-BEAM

A simple model of a built-up type of wing structure is the I-beam with wide flanges. The present section is concerned with the transient temperature distribution associated with the heating of such a beam by convective heat transfer into the outer surfaces of the flanges.

The following assumptions are made:

(1) The environment temperature and convective heat transfer coefficient are uniform over the outer surfaces of the flanges, the latter being constant with time as well.

(2) The temperature in the beam is initially uniform.

(3) The flow of heat takes place entirely in directions parallel to planes representing cross-sections of the beam. That is, the heat loss out of the ends of the beam may be neglected, so that the temperature distribution at any instant is the same in all cross-sections of the beam.

(4) The flanges and web are sufficiently thin that temperature variation through their thickness may be neglected.

(5) The inner surfaces of the flanges and both surfaces of the web are insulated, so that heat transfer between parts of the beam takes place by conduction only.

(6) There is no heat transferred through the edges of the flanges.

(7) Variation of the thermal properties of the material with temperature may be neglected.

The problem thus reduces to one of one-dimensional heat flow in the flange and in the web.

A simplified treatment of this problem has been given by Hoff and Torda[5], in which the heat loss from the flanges into the web is neglected in

the determination of the transient temperature variation in the flanges, and this temperature variation is then applied as a boundary condition on the web. A more refined analysis, based on assumptions which are the same as those made here, has been given by Pohle and Oliver.[6] In the present work, the results of this previous work are extended considerably and information is provided on the effect of a finite period of build-up of the environment temperature.

The present analysis satisfies the transition conditions at the joints between the flanges and web exactly. The beam is assumed initially to be built-up, in the sense that the flanges and web are not integral but are connected by screws or pins or some similar arrangement, leaving a surface between the flange and web across which there may be effectively a temperature discontinuity. The solution for a beam with integral flange and web is then obtained as a special case.

The coordinates and dimensions of the beam cross-section are shown in Figure 13. The depth of the beam is measured between the middle surfaces of the flanges.

The partial differential equations for the temperature in the flanges and web are respectively,

$$\frac{\partial T_f}{\partial t} = \kappa \frac{\partial^2 T_f}{\partial x^2} + \kappa \frac{h}{\delta_f k} (T_e - T_f) \tag{19}$$

$$\frac{\partial T_w}{\partial t} = \kappa \frac{\partial^2 T_w}{\partial y^2} \tag{20}$$

Taking symmetry into account, it is necessary to consider the flange only in the range $0 \leq x \leq b$, and the web only in the range $0 \leq y \leq s$ The boundary and initial conditions may now be written,

(1) At $x = b$, $\quad \frac{\partial T_f}{\partial x} = 0$

(2) At $y = 0$, $\quad \frac{\partial T_w}{\partial y} = 0$

(3) At $x = 0$, $y = s$, $\quad 2 k \delta_f \frac{\partial T_f}{\partial x} = h_j \delta_w (T_f - T_w) = k \delta_w \frac{\partial T_w}{\partial y}$

(4) At $t = 0$, $\quad T_f = T_w = T_i$

Equations (19) and (20) may be put into the following non-dimensional form ,

$$\frac{\partial \phi_f}{\partial \tau} = \frac{\partial^2 \phi_f}{\partial \xi^2} - \lambda (\phi_f - \phi_e) \tag{21}$$

$$\frac{\partial \phi_w}{\partial \tau} = \frac{\partial^2 \phi_w}{\partial \eta^2} \tag{22}$$

and the boundary and initial conditions become

(1) At $\xi = \frac{b}{s}$, $\qquad \frac{\partial \phi_f}{\partial \xi} = 0$

(2) At $\eta = 0$, $\qquad \frac{\partial \phi_w}{\partial \eta} = 0$

(3) At $\xi = 0$, $\eta = 1$, $\qquad 2\gamma \frac{\partial \phi_f}{\partial \xi} = \lambda_j (\phi_f - \phi_w) = \frac{\partial \phi_w}{\partial \eta}$

(4) At $\tau = 0$, $\qquad \phi_f = \phi_w = 1$

As in the case of the plate, a finite difference numerical method was used in the solution of Equations (21) and (22). The method is described in Appendix B.

A program of computations was carried out on the Whirlwind I computer for a variety of values of the parameters λ, γ and τ_g, the time history of the environment temperature being assumed to have the form shown in Figure 2. The influence of the parameters λ and γ on the maximum temperature differential in the beam is shown in Figure 14 for the case, $\tau_g = 0$. The width of the flange was taken to be twice the depth of the web in all cases. The web and flange were assumed to be integral.

The curves for $\gamma = \infty$ correspond to the simplified analysis of Hoff and Torda.[5] The influence of the parameter γ is seen to be substantial at intermediate values of the parameter λ, and such as to make the results of Hoff and Torda unconservative.

The influence of the gradient time, τ_g, is shown in Figure 15 for the case, $\gamma = 1$. The results are expressed as a factor modifying the

results obtained for the case, $\tau_g = 0$. The effect of τ_g is seen to be greatest at intermediate values of λ .

The influence of the parameters γ and λ on the temperature distribution at the time of maximum temperature differential is shown in Figures 16 and 17 respectively for the case, $\tau_g = 0$.

V. THERMAL STRESSES IN A WIDE-FLANGED I-BEAM OF INFINITE LENGTH

The thermal stresses due to the transient temperature distribution in the I-beam described in the preceding section are now considered.

The beam is first assumed to be infinitely long. Since the temperature distribution is the same in all cross-sections of the beam and is symmetrical about the x and y axes (Figure 13), it follows that cross-sections must remain plane and parallel during heating of the beam.

The assumption of thinness of the flange and web and the fact that the temperature is uniform through their thickness results in a condition of plane stress in each.

As the beam is free to deform within any cross-section, the only stresses present will be in the longitudinal direction, that is, $\sigma_x = \sigma_y = 0$. It is easily shown that under these circumstances the longitudinal stress is given by

$$\sigma_z = -\alpha E (T - T_i) + C \tag{23}$$

where C is a function of time only, and is determined from the condition that the net force on any cross-section is zero, or

$$2\int_{-b}^{b} \sigma_{z_f}\, dx + \delta_w \int_{-s}^{s} \sigma_{z_w}\, dy = 0 \tag{24}$$

yielding,

$$C = \alpha E \left[\frac{2\delta_f}{2b\delta_f + s\delta_w} \int_0^b (T_f - T_i)\, dx - \frac{\delta_w}{2b\delta_f + s\delta_w} \int_0^s (T_w - T_i)\, dy \right] \tag{25}$$

Equation (23) may be written in the non-dimensional form

$$\frac{\sigma_{z_f}}{\alpha E (T_{e_r} - T_i)} = \phi_f(\xi) - A \tag{26}$$

$$\frac{\sigma_{z_w}}{\alpha E (T_{e_r} - T_i)} = \phi_w(\eta) - A \tag{27}$$

$$\frac{1}{\gamma\omega + 1} \int_0^1 \phi_w(\eta)\, d\eta \tag{28}$$

$$\frac{\sigma_{z_f}}{\alpha E (\Delta T)_{max.}} = \frac{1}{(\Delta\phi)_{max.}} \left\{ \phi_f(\xi) - A \right\} \tag{29}$$

$$\frac{\sigma_{z_w}}{\alpha E (\Delta T)_{max.}} = \frac{1}{(\Delta\phi)_{max.}} \left\{ \phi_w(\eta) - A \right\} \tag{30}$$

It should be noted that ξ is defined differently here than in the preceding section.

It is seen that

$$(\sigma_{z_w})_{\eta=0} - (\sigma_{z_f})_{\xi=1} = \alpha E (\Delta T)_{max.} \tag{31}$$

The temperature data of the preceding section have been used to compute stress data for the wide-flanged I-beam. In addition to the parameters λ, γ and τ_g, the parameter ω is now significant. While the temperature distributions were computed for $\omega = 2$, it is in most cases sufficiently accurate to use these distributions for other flange widths, cutting the distribution curve off at the appropriate point for a narrower flange and extending it horizontally for a wider flange. This procedure introduces the greatest error at low values of λ, where the effect of heat loss to the web is felt far out on the flange.

Figure 18 shows, for $\tau_g = 0$, how the stress range in the beam at the time of maximum temperature differential divides between maximum tensile stress and maximum compressive stress. The maximum tensile stress occurs at the middle of the web, while the maximum compressive stress occurs at the edge of the flange. The curves are identified in groups of constant ratio of flange to web cross-sectional area, $A_f / A_w = 2\gamma\omega$.

In relating the maximum stresses directly to flight parameters, and in comparing their values as obtained by the simplified method of Hoff and Torda[5] with those obtained by the more exact method, it is preferable to use the quantities defined in Equations (26) and (27). These are shown plotted in Figure 19 for $\tau_g = 0$ and $A_f / A_w = 8$. It was found that the simplified analysis yields substantially unconservative values for maximum compressive stress in all cases, and values for maximum tensile stress which are slightly conservative at large values of λ and which may be either conservative or unconservative at low values of λ, depending upon the values of γ and A_f / A_w.

The effect of gradient time on the maximum values of $\dfrac{\sigma_z}{\alpha E (\Delta T)_{max.}}$ was found to be slight in all cases. In the extreme case of $\lambda = 100$, the

maximum tensile stress is increased about 1.5 percent and the maximum compressive stress is decreased about 8 percent when the relative gradient time $(\tau_g)_r$ is increased from 0 to 8.

In any practical application the stress may be determined by the use of Figure 18 in conjunction with the temperature data of the preceding section.

VI. THERMAL STRESSES IN A WIDE-FLANGED I-BEAM OF FINITE LENGTH

The effect of free ends on the thermal stress distribution in the wide-flanged I-beam is now considered. The assumptions regarding temperature distribution remain unchanged. The coordinate axes of the beam are shown in Figure 20. The origin is at the center of the beam.

The flanges and web are again assumed to be sufficiently thin that stresses normal to their surface may be neglected. Stresses in the plane of the flange and web are considered to be uniform through their respective thicknesses. Deflections of the flange and web normal to their respective planes are assumed not to occur. This precludes buckling of the flanges under compressive stress.

On the basis of these assumptions, the problem reduces to one of plane stress in the flange and web, with the satisfaction of boundary conditions at the joints connecting them and at their free edges.

The stress distribution may be found conveniently as the superposition of two component stress distributions. The first component stress distribution is that corresponding to the beam of infinite length. The second component stress distribution is that necessary to result in satisfaction of the boundary conditions on the ends of the beam, and is obtained by applying to the ends of the beam a longitudinal load distribution equal and opposite in sign to the stress distribution in a cross-section of the infinite beam. Since this load distribution is self-equilibrating, its effect will, according to Saint-Venant's principle, be large only near the ends of the beam, and will diminish rapidly with increasing distance from the ends of the beam.

The second component stress distribution is now analyzed by the methods of the mathematical theory of elasticity for plane stress.

The boundary conditions are as follows:

(1) At $\xi = \pm 1$, $\quad \sigma_{x_f} = \tau_{xz_f} = 0$

(2) At $\zeta = \pm 1$, $\quad \sigma_{z_f} = \sigma_{o_f}$

$$\sigma_{z_w} = \sigma_{o_w}$$

$$\tau_{xz_f} = \tau_{yz_w} = 0$$

(3) At $\xi = 0$, $\eta = \pm 1$, $\quad \tau_{yz_w} = 2\gamma\tau_{xz_f}$

where σ_{o_f} and σ_{o_w} are the negative of the longitudinal stresses in the flange and web, respectively, of the beam of infinite length.

In an exact treatment of the problem, two additional conditions would have to be satisfied at the joint between flange and web. The first of these is the continuity condition that longitudinal strain in the flange and web should be equal at this joint. In terms of stress, this condition may be written as follows:

(4) At $\xi = 0$, $\eta = \pm 1$, $\quad \sigma_{z_w} = \sigma_{z_f} - \nu\sigma_{x_f}$

The second additional condition arises from the fact that the curve of displacement of an originally straight line in the x-direction in the flange is discontinuous in slope at x = 0, due to the shear flow into the flange from the web. Because of this discontinuity, it is convenient to treat the two halves of the flange lying in the positive and negative directions of x separately, and to define a condition establishing continuity between them. Such

a condition is one requiring that, along a line in the flange coincident with the joint,

$$\frac{\partial^2 u_f}{\partial z^2} = 0$$

where u_f represents displacement in the x-direction. This condition may be expressed in terms of stresses as follows,

(5) At $\xi = 0$, $$\frac{\mu}{\psi} \frac{\partial \tau_{xz_f}}{\partial \zeta} = \frac{\partial \sigma_{z_f}}{\partial \xi}$$

In plane stress problems, the state of stress in the body may be described by means of a single scalar function of the space coordinates. Such a function, known as the "Airy stress function", denoted here by ϕ, is defined in the x, z plane for the case of zero body forces by[7],

$$\sigma_x = \frac{\partial^2 \phi}{\partial z^2} \qquad \sigma_z = \frac{\partial^2 \phi}{\partial x^2} \qquad \tau_{xz} = -\frac{\partial^2 \phi}{\partial x \partial z} \tag{32}$$

It can be seen that ϕ, as defined, satisfies the equations of equilibrium. In order to represent the true state of stress in the body, ϕ must also satisfy the compatibility equation and the boundary conditions.

In the present problem it is necessary to establish separate functions ϕ_w and ϕ_f in the web and flange regions respectively. The boundary conditions at the free edges, as well as at the joint between flange and web, would have to be satisfied in an exact solution of the problem.

It is possible to obtain such an exact solution only in the simplest cases, and in the present case it would hardly be feasible. It is, consequently,

necessary to resort to a method yielding an approximate solution. Such a method is provided by the Ritz procedure of expressing the function ϕ as a linear combination of assumed functions in proportions which are initially unknown. That is,

$$\phi = \phi_0 + a_1 \phi_1 + a_2 \phi_2 + \text{-----}$$

where ϕ_0, ϕ_1, ϕ_2 . . . . are the assumed functions and a_1, a_2, . . . the unknown multipliers. The unknowns may then be determined by setting up an expression for the strain energy in the body as a function of these unknowns and minimizing it with respect to each unknown in turn, yielding a set of simultaneous linear algebraic equations which may be readily solved. This is an application of the so-called "principle of least work". The degree of approximation will be determined by the facility with which the assumed stress functions can be superposed to approximate the true state of stress in the body, and will consequently depend upon the nature of the true stress distribution, the nature of the assumed functions and the number of functions assumed.

It was found, after considerable investigation, that assumed functions in the form of polynomial expressions would be most suitable for the satisfaction of boundary conditions and convenient in subsequent mathematical manipulations. In consequence, the following series expressions for the stress functions in the flange and web regions were chosen,

$$\phi_f = \phi_{0f} + \sum_{m=0}^{p} \sum_{n=0}^{p} A_{mn} (\xi - 1)^2 (\zeta^2 - 1)^2 \xi^m \zeta^{2n} \qquad (33)$$

where

$$\phi_{0f} = b^2 \int\int \sigma_{0f} \, d\xi \, d\xi$$

and

$$\phi_w = \phi_{o_w} + \sum_{m=o}^{p} \sum_{n=o}^{p} B_{mn} (\eta^2-1)(\zeta^2-1)^2 \eta^{2m} \zeta^{2n} \qquad (34)$$

where

$$\phi_{o_w} = s^2 \iint \sigma_{o_w} \, d\eta \, d\eta$$

It should be noted that the expression for ϕ_f, as written, applies only in the range of positive ξ. This is unavoidable for reasons discussed previously in connection with the development of boundary condition (5). Because of symmetry, the strain energy in the two halves of the flange will be equal, so that only one side need be considered in the energy minimization process.

Continuity between the two halves could be established on an exact basis by the application of boundary condition (5). It has been found, however, and will be demonstrated later, that an exact satisfaction of boundary conditions (4) and (5) greatly increases the difficulty of obtaining a satisfactory solution with a reasonable number of assumed functions.

Even if boundary conditions (4) and (5) are not applied explicitly in the analysis, the energy minimization process will tend toward their satisfaction. This follows from the fact that minimization of the strain energy on an exact basis leads to the true stress distribution only if the forces applied at the boundaries of the various regions do not change during the variation process or if no net work is done by changes in these forces (reference 7, page 150). The first of these conditions is seen to be automatically satisfied at the free edges of the beam by each of the assumed stress functions individually. At the joint between flange and web the shear forces will be equal in

magnitude and opposite in direction in each because of boundary condition (3). If changes in these shear forces are to do no net work, the displacements through which they act must be equal. Consequently, this provides for the satisfaction of boundary condition (4). The assumed functions provide for stresses σ_x in the flange at its centerline ($\xi = 0$), and consequently changes in these stresses will do no work only if the displacement through which they act is zero. This, in turn, provides for the satisfaction of boundary condition (5).

On the basis of these considerations, the analysis now proceeds, with boundary conditions (4) and (5) eliminated from explicit consideration. Boundary conditions (1) and (2) are seen to be satisfied by the assumed stress functions. It remains now to establish relations between the unknown coefficients A_{mn} and B_{mn} for the satisfaction of boundary condition (3).

From Equations (32), (33) and (34), the expressions for stress may be written as follows,

$$\sigma_{z_f} = \sigma_{o_f} + \frac{\psi^2}{\ell^2} \sum_{m=0}^{p} \sum_{n=0}^{p} A_{mn} (\zeta^2 - 1)^2 \zeta^{2n} \{(m+2)(m+1)\xi^m - 2m(m+1)\xi^{m-1} + m(m-1)\xi^{m-2}\} \tag{35}$$

$$\sigma_{x_f} = \frac{2}{\ell^2} \sum_{m=0}^{p} \sum_{n=0}^{r} A_{mn} (\xi - 1)^2 \xi^m \{(n+2)(2n+3)\zeta^{2n+2} - 2(2n+1)(n+1)\zeta^{2n} + n(2n-1)\zeta^{2n-2}\} \tag{36}$$

$$\tau_{xz_f} = -\frac{2\psi}{\ell^2} \sum_{m=0}^{p} \sum_{n=0}^{p} A_{mn} (\zeta^2 - 1)\{(2+n)\zeta^{2n+1} - n\zeta^{2n-1}\}(\xi - 1) \{(m+2)\xi^m - m\xi^{m-1}\} \tag{37}$$

$$\sigma_{z_w} = \sigma_{o_w} + \frac{2\psi^2\omega^2}{\ell^2} \sum_{m=0}^{p} \sum_{n=0}^{p} B_{mn} (\zeta^2-1)^2 \zeta^{2n} \left\{ (m+1)(2m+1)\eta^{2m} - m(2m-1)\eta^{2m-2} \right\} \tag{38}$$

$$\sigma_{y_w} = \frac{2}{\ell^2} \sum_{m=0}^{p} \sum_{n=0}^{p} B_{mn} (\eta^2-1)\eta^{2m} \left\{ (n+2)(2n+3)\zeta^{2n+2} - 2(n+1)(2n+1)\zeta^{2n} + n(2n-1)\zeta^{2n-2} \right\} \tag{39}$$

$$\tau_{yz_w} = -\frac{4\psi\omega}{\ell^2} \sum_{m=0}^{p} \sum_{n=0}^{p} B_{mn} (\zeta^2-1) \left\{ (2+n)\zeta^{2n+1} - n\zeta^{2n-1} \right\} \left\{ (m+1)\eta^{2m+1} - m\eta^{2m-1} \right\} \tag{40}$$

in which terms with negative exponents should be disregarded.

Introducing the appropriate expressions into boundary condition (3), the following relation is obtained,

$$\frac{\gamma}{\omega} \sum_{n=0}^{p} (2A_{on} - A_{in}) \left\{ (2+n)\zeta^{2n+3} - 2(1+n)\zeta^{2n+1} + n\zeta^{2n-1} \right\} = -\sum_{m=0}^{p} \sum_{n=0}^{p} B_{mn} \left\{ (2+n)\zeta^{2n+3} - 2(1+n)\zeta^{2n+1} + n\zeta^{2n-1} \right\} \tag{41}$$

Since Equation (41) is an indentity, a set of relations between the unknown coefficients could be established by equating coefficients in like powers of ζ . However, these relations can be established more simply by recognizing that, for any given η , the polynomials in ζ are identically the same on both sides of the equation, and equating coefficients of these polynomials. Thus,

$$\frac{\gamma}{\omega}(2A_{on} - A_m) = -\sum_{m=o}^{p} B_{mn} \qquad (n = 0,1,2 \ldots p) \qquad (42)$$

Equation (42) provides $p + 1$ relations which permit the expression of $p + 1$ of the unknowns as linear functions of the remaining unknowns in the total set of $2(p + 1)^2$ unknowns. The resulting linear relations may be put in matrix form as follows,

$$\{b\} = [D]\{a\} \qquad (43)$$

where $\{a\}$ and $\{b\}$ are column matrices of the independent and dependent unknowns respectively, and $[D]$ is a rectangular matrix which depends only upon the parameters γ and ω . For example, in the simple case, $p = 1$,

$$\{a\} = \begin{Bmatrix} A_{00} \\ A_{01} \\ A_{10} \\ A_{11} \\ B_{00} \\ B_{01} \end{Bmatrix} \qquad \{b\} = \begin{Bmatrix} B_{10} \\ B_{11} \end{Bmatrix}$$

$$[D] = \begin{bmatrix} -2\frac{\gamma}{\omega} & 0 & \frac{\gamma}{\omega} & 0 & -1 & 0 \\ 0 & -2\frac{\gamma}{\omega} & 0 & \frac{\gamma}{\omega} & 0 & -1 \end{bmatrix}$$

Applying the following expression (reference 7, page 152) for strain energy in a flat plate of thickness δ, subjected to stress only in its own plane,

$$V = \frac{\delta}{2E}\iint \left\{ \sigma_x^2 + \sigma_z^2 - 2\nu\sigma_x\sigma_z + 2(1+\nu)\tau_{xz}^2 \right\} dx\, dz$$

the strain energy in the beam may be expressed as follows,

$$V = \frac{4b\ell\delta_f}{E}\int_0^1\int_0^1 \left\{ \sigma_{x_f}^2 + \sigma_{z_f}^2 - 2\nu\sigma_{x_f}\sigma_{z_f} + 2(1+\nu)\tau_{xz_f}^2 \right\} d\xi\, d\zeta$$

$$+ \frac{2s\ell\delta_w}{E}\int_0^1\int_0^1 \left\{ \sigma_{y_w}^2 + \sigma_{z_w}^2 - 2\nu\sigma_{y_w}\sigma_{z_w} + 2(1+\nu)\tau_{yz_w}^2 \right\} d\eta\, d\zeta \quad (44$$

stitution of Equations (35) to (40) inclusive into Equation (44),

ion of the linear relations given in Equation (43), results in a quadratic form in the independent unknown coefficients plus a sum of linear terms in these unknowns. Minimization of the strain energy involves application of the condition

$$\frac{\delta V}{\delta a_n} = 0 \qquad (n = 1, 2 \ldots\ldots (p+1)(2p+1)) \quad (45)$$

where $\frac{\delta V}{\delta a_n}$ denotes a partial differentiation with respect to each of the independent unknown coefficients, a_n . Equation (45) may be written as follows,

$$\frac{\delta V}{\delta a_n} = \frac{\partial V}{\partial a_n} + \sum_{m=1}^{p+1} \frac{\partial V}{\partial b_m} \frac{\partial b_m}{\partial a_n} \qquad (n = 1, 2 \ldots . (p+1)(2p+1)) \quad (46)$$

where b_m are the dependent unknown coefficients and $\frac{\partial V}{\partial a_n}$ and $\frac{\partial V}{\partial b_m}$ denote partial differentiations in which all of the unknowns are regarded as independent.

Equation (46) may be written in the matrix form,

$$\left\{\frac{\delta V}{\delta a}\right\} = \left\{\frac{\partial V}{\partial a}\right\} + [D]' \left\{\frac{\partial V}{\partial b}\right\} = 0 \quad (47)$$

where $[D]'$ is the transpose of the matrix $[D]$ defined in Equation (43).

The matrices $\left\{\frac{\partial V}{\partial a}\right\}$ and $\left\{\frac{\partial V}{\partial b}\right\}$ may be developed in the following partitioned matrix form,

$$\begin{Bmatrix} \left\{\frac{\partial V}{\partial a}\right\} \\ \left\{\frac{\partial V}{\partial b}\right\} \end{Bmatrix} = \begin{bmatrix} [K_1] & [K_2] \\ [K_3] & [K_4] \end{bmatrix} \begin{Bmatrix} \{a\} \\ \{b\} \end{Bmatrix} + \begin{Bmatrix} \{d\} \\ \{e\} \end{Bmatrix}$$

which reduces to the matrix equations,

$$\left\{\frac{\partial V}{\partial a}\right\} = [K_1]\{a\} + [K_2]\{b\} + \{d\} \quad (48)$$

$$\left\{\frac{\partial V}{\partial b}\right\} = [K_3]\{a\} + [K_4]\{b\} + \{e\} \quad (49)$$

Substitution of Equation (43) into Equations (48) and (49), and introduction of the result into Equation (47), finally yields the matrix equation,

$$\left([K_1] + [K_2][D] + [D]'[K_3] + [D]'[K_4][D]\right)\{a\} = -\{d\} - [D]'\{e\} \tag{50}$$

which is seen to represent a set of $(p + 1)(2p + 1)$ simultaneous linear algebraic equations which may be solved for the coefficients a_n, which may then, in turn, be substituted into Equation (43) to yield the coefficients, b_m. Finally, substitution of the coefficients into Equations (35) to (40) inclusive yields the stress distributions.

The matrices $[K_1]$, $[K_2]$, $[K_3]$, $[K_4]$, $\{d\}$ and $\{e\}$ may be determined most conveniently by differentiating Equation (44) with respect to each of the unknowns before integration. Thus,

$$\frac{\partial V}{\partial A_{rs}} = \frac{8bl\delta_f}{E}\int_0^1\int_0^1 \left\{ \sigma_{x_f}\frac{\partial \sigma_{x_f}}{\partial A_{rs}} + \sigma_{z_f}\frac{\partial \sigma_{z_f}}{\partial A_{rs}} - \nu\sigma_{x_f}\frac{\partial \sigma_{z_f}}{\partial A_{rs}} - \nu\sigma_{z_f}\frac{\partial \sigma_{x_f}}{\partial A_{rs}} + 2(1+\nu)\tau_{xz_f}\frac{\partial \tau_{xz_f}}{\partial A_{rs}} \right\} d\xi\, d\zeta \tag{51}$$

and a similar expression is obtained for $\frac{\partial V}{\partial B_{rs}}$

Substitution of Equations (35), (36) and (37) into Equation (51), and integration as indicated, leads to an expression of the form,

$$\frac{\partial V}{\partial A_{rs}} = \frac{8\gamma\delta_w}{\ell^2\psi E}\left[\sum_{m=0}^{p}\sum_{n=0}^{p}\left\{4C_{mn}^{rs}\left(\sigma_{x_f}\frac{\partial\sigma_{x_f}}{\partial A_{rs}}\right) + \psi^4 C_{mn}^{rs}\left(\sigma_{z_f}\frac{\partial\sigma_{z_f}}{\partial A_{rs}}\right)\right.\right.$$

$$-2\nu\psi^2 C_{mn}^{rs}\left(\sigma_{x_f}\frac{\partial\sigma_{z_f}}{\partial A_{rs}}\right) - 2\nu\psi^2 C_{mn}^{rs}\left(\sigma_{z_f}\frac{\partial\sigma_{x_f}}{\partial A_{rs}}\right)$$

$$\left.\left. + 8(1+\nu)\psi^2 C_{mn}^{rs}\left(\tau_{xz_f}\frac{\partial\tau_{xz_f}}{\partial A_{rs}}\right)\right\}A_{mn} + \ell^2\psi^2 C_c^{rs}\left(\sigma_{z_f}\frac{\partial\sigma_{z_f}}{\partial A_{rs}}\right)\right] \quad (52)$$

where $C_{mn}^{rs}\left(\sigma_{x_f}\frac{\partial\sigma_{x_f}}{\partial A_{rs}}\right)$, etc., are non-dimensional coefficients which depend only upon the assumed functions, while the constants $C_c^{rs}\left(\sigma_{z_f}\frac{\partial\sigma_{z_f}}{\partial A_{rs}}\right)$ are functions of the applied loading and are dimensional. The derivative $\frac{\partial V}{\partial B_{rs}}$ may be expressed in a similar form. Development of the expressions for the various coefficients and constants is too lengthy for inclusion in the present paper.

The preceding analysis was applied to the case, $\psi = 3$, $\omega = 2$, $\nu = 1$. The loading corresponded to a condition of thermal stress resulting from transient heating as described in Section IV, with $\lambda = 3.5$, $\tau_g = 0$. The temperature distribution was that corresponding to the maximum temperature differential between the edges of the flange and the middle of the web. The stress distribution for the case of an infinitely long beam was first determined by the method of Section V, the actual stress levels being based on a maximum stress range of 10,000 psi in the beam cross-section. This stress distribution was then reversed in sign and applied as an external loading on the ends of the finite beam to determine the end effect.

Three different analyses were performed. Two of these were based on the method developed above, without explicit satisfaction of boundary conditions (4) and (5), and are termed "simplified analyses". One involved the use of a total of eight terms in the two stress function expressions ($m = 0, 1$, $n = 0, 1$) and the other a total of eighteen terms ($m = 0, 1, 2$, $n = 0, 1, 2$).

In the third analysis, boundary conditions (4) and (5) were satisfied explicitly, and a total of thirty-two terms ($m = 0, 1, 2, 3$, $n = 0, 1, 2, 3$) were used in the stress function expressions. The details of this analysis, termed the "comprehensive analysis", are not included in the present paper because of space limitations.

The results obtained from the three analyses are shown in Figures 21 and 22. Figure 21 shows that even the eight term approximation using the simplified analysis yields a more accurate result than the much lengthier comprehensive analysis. This is further borne out by the shear stress distributions shown in Figure 22, where the large reversal of stress in the middle portion of the beam obtained from the comprehensive analysis appears highly unlikely from physical considerations. It is more likely that no reversal occurs and that the shear stress is close to zero over a substantial length of the middle portion of the beam. The results given by the simplified analyses seem to be tending toward such a distribution. In connection with the peak value of shear stress near the end of the beam, which is the result of greatest significance, it is difficult to tell the extent to which the approximate results of the simplified method have approached the exact value.

The failure of the comprehensive analysis to provide a satisfactory result can be attributed to the fact that the exact satisfaction of boundary conditions (4) and (5) with a limited number of terms forces a considerable distortion of the stress distribution curves in the remainder of the beam.

VII. EXPERIMENTAL INVESTIGATION OF THE TRANSIENT TEMPERATURE DISTRIBUTION AND THERMAL STRESSES IN A WIDE-FLANGED I-BEAM

The theory of the preceding sections was checked experimentally by means of the apparatus shown in Figure 23. The specimen used was built up of 1/4 inch steel plate, with the web-flange joints brazed in order to provide an unimpeded path for heat flow from the flanges into the web. The remaining dimensions of the beam were 2ℓ = 30 inches, $2b$ = 10 inches, $2s$ = 5 inches.

Convective heat transfer into the outer faces of the flanges was simulated by the transfer of heat from large heated aluminum blocks across a small air gap (.007 inch). The proper gap was maintained by means of suitably located spacers, and the effect of flange warpage was eliminated by providing an initial concave outward curvature and exerting enough pressure across the two heating blocks to bend the flanges back to a flat shape.

The blocks were preheated by means of electric resistance rods, and then brought up to the specimen and clamped tightly. The surface temperature of the blocks was intended to simulate an environment temperature varying as a step function, and the thermal conductance of the air gap was intended to simulate the convective heat transfer coefficient. As heat flowed across the gap, there was found to be a drop in the surface temperature of the block, thus violating the assumption of a step function variation of environment temperature. However, there was simultaneously an increase in the conductivity of the air in the gap due to a rise in its temperature, and the two effects were found to be largely compensating. The value of the parameter λ was estimated to be 2.42.

Temperature was measured at selected stations on the inner faces of the flanges and on the web surfaces by means of electric resistance gages and stress was measured at similar locations by temperature-compensating wire resistance strain gages. Both temperature and stress were recorded continuously by means of oscillograph equipment.

The variation of temperature with time, as determined both theoretically and experimentally, is shown in Figure 24 for gage locations in the middle cross-section of the beam. The corresponding longitudinal stress variations are shown in Figure 25. The temperature and logitudinal stress distributions in the middle cross-section at the time of maximum temperature differential are shown in Figures 26 and 27 respectively.

Shear stress was measured by means of strain rosettes at locations on the surface of the web near one end of the beam and close to the web-flange joint. The experimental values obtained at the time of maximum temperature differential are shown in Figure 28 along with the corresponding theoretical distribution as obtained from the "simplified analysis" of Section VI, using eighteen terms. The experimental results indicate that the peak value of shear stress occurs closer to the end of the beam than is indicated by the approximate theoretical result, and is slightly lower in value.

The results in general indicate good agreement between theory and experiment, and encourage confidence in the theoretical method.

APPENDIX A

FINITE DIFFERENCE PROCEDURE FOR SOLUTION OF THE PLATE HEATING PROBLEM

An approximate solution for the transient temperature distribution in the plate, for an arbitrary variation of the environment temperature with time, may be obtained by the application of the calculus of finite differences.

The thickness of the plate is divided into increments of equal length, $\Delta\xi$, and the time domain into equal increments, $\Delta\tau$ This establishes a set of equally spaced stations in the plate.

Applying the usual methods of the calculus of finite differences, the following relation may be set up for the temperature at an interior station (reference 2, page 375),

$$\phi_{n_{\tau+\Delta\tau}} = \frac{1}{M}\phi_{n-1_\tau} + \left(1 - \frac{2}{M}\right)\phi_{n_\tau} + \frac{1}{M}\phi_{n+1_\tau} \qquad \text{(A-1)}$$

where $M = (\Delta\xi)^2/\Delta\tau$. The subscript n refers to the station. It is taken as 0 at the heated surface and numbered 1, 2, 3, etc. toward the insulated surface.

It has been found that all three coefficients in Equation (A-1) should be positive; otherwise, convergence difficulties may be encountered. This sets a lower limit of 2 on the value of M . In general, a somewhat larger value, such as 2.5 or 3, is preferable.

The temperature at the insulated surface may be determined by treating it as a plane of symmetry, so that

$$\phi_{n_{\tau+\Delta\tau}} = \frac{2}{M}\phi_{n-1_\tau} + \left(1 - \frac{2}{M}\right)\phi_{n_\tau} \qquad \text{(A-2)}$$

The usual procedure for determining the temperature at the heated surface involves the establishment of a heat balance for a block extending from that surface halfway to the first interior station, leading to the relation (reference 2, page 376),

$$\phi_{o_{\tau+\Delta\tau}} = \frac{2N}{M}\phi_{e_\tau} + \left(1 - \frac{2N}{M} - \frac{2}{M}\right)\phi_{o_\tau} + \frac{2}{M}\phi_{1_\tau} \qquad \text{(A-3)}$$

where $N = \lambda \Delta \xi$. To insure convergence, it is again necessary that all coefficients be positive (reference 8, page 129), leading to the requirement that $M > 2N+2$.

When N is large, as it may be for large values of λ , satisfaction of this requirement may lead to a value of M which is too large for practical computation. A further objection to the procedure is that the temperature gradient is expressed in terms of only two ordinates, which may in some cases introduce substantial errors, particularly when λ is large and the environment temperature changes abruptly.

An alternative procedure for determining ϕ_o which avoids or mitigates these difficulties was adopted in the present work. It represents a refinement of a method presented in reference 8, page 129. Expressing the temperature gradient at the heated surface in finite difference form, using first and second differences[9],

$$\left(\frac{\partial \phi}{\partial \xi}\right)_{\xi=1} = \frac{1}{\Delta\xi}\left(1.5\,\phi_0 - 2.0\,\phi_1 + 0.5\,\phi_2\right) \qquad \text{(A-4)}$$

and substituting this expression into boundary condition (2) of Section II, leads to the relation,

$$\phi_{o_\tau} = \frac{2}{N+1.5}\phi_{1_\tau} - \frac{0.5}{N+1.5}\phi_{2_\tau} + \frac{N}{N+1.5}\phi_{e_\tau} \qquad \text{(A-5)}$$

where N is as defined previously.

An apparent disadvantage of this procedure is that the increment in ϕ_o during the first time interval is independent of $\Delta\tau$. If this increment is small, it may be expected that after a few cycles ϕ_o will adjust to a realistic value and a satisfactory result will be obtained. On the other hand, if it is large, it may be expected that a substantial error will result. This will occur when N is large and the environment temperature changes rapidly or abruptly. For any given value of λ, N may, of course, be reduced by taking $\Delta\xi$ smaller, but only at the expense of a rapid increase in the volume of computations, since $\Delta\tau$ may also have to be decreased because of the restriction on M.

A more satisfactory remedy involves the matching of the first increment in ϕ_o as given by Equation (A-5), with the true value of this increment by an appropriate choice of $\Delta\tau$. While this true value is not known, it can be approximated satisfactorily by the corresponding value for a semi-infinite slab. The solution for the surface temperature in the latter case when the environment temperature has a step function variation, is given by (reference 4, page 53),

$$\phi = e^{\lambda^2\tau}\,\mathrm{erfc}\,(\lambda\sqrt{\tau}) \qquad \text{(A-6)}$$

where erfc is the complementary error function and is widely tabulated. Thus

$$\phi_{o_{\tau=\Delta\tau}} = e^{\lambda^2\Delta\tau}\,\mathrm{erfc}\left(\lambda\sqrt{\Delta\tau}\right) \tag{A-7}$$

The corresponding value for the plate, as given by Equation (A-5), is

$$\phi_{o_{\tau=\Delta\tau}} = \frac{1.5}{N+1.5} \tag{A-8}$$

and a value for $\Delta\tau$ may be determined by equating the right-hand sides of Equations (A-7) and (A-8). This value of $\Delta\tau$ may be applied also when the environment temperature does not vary as a step function, although, when the environment temperature is initially the same as the plate temperature and does not rise very rapidly, the choice of $\Delta\tau$ will not be critical and a satisfactory result can be expected for any reasonably small $\Delta\tau$.

APPENDIX B

FINITE DIFFERENCE PROCEDURE FOR SOLUTION OF THE I-BEAM HEATING PROBLEM

The finite difference procedure used in solving for transient temperatures in the wide-flanged I-beam is somewhat similar to that described previously for the plate.

Stations are selected in the beam cross-section spaced at equal intervals $\Delta\xi$ along the flange and $\Delta\eta$ along the web such that the flange width and web depth are even multiples of $\Delta\xi$ and $\Delta\eta$ respectively. These stations are designated by 0 at the web-flange joint, 1, 2, 3, etc. in the flange, and -1, -2, -3, etc. in the web. When the web and flange are not integral, station 0 is designated as +0 in the flange and -0 in the web.

When expressed in finite difference form, Equation (21) may be reduced to the following relation,

$$\phi_{n_{\tau+\Delta\tau}} = F_1\,\phi_{n-1_\tau} + F_2\,\phi_{n_\tau} + F_3\,\phi_{n+1_\tau} + F_4\,\phi_{e_\tau} \qquad \text{(B-1)}$$

where

$$F_1 = F_3 = \frac{1}{M_f}$$

$$F_2 = 1 - \frac{2}{M_f} - \frac{\lambda(\Delta\xi)^2}{M_f}$$

$$F_4 = \frac{\lambda(\Delta\xi)^2}{M_f}$$

with $$M_f = \frac{(\Delta\xi)^2}{\Delta\tau}$$

Similarly, for the web,

$$\phi_{n_{\tau+\Delta\tau}} = G_1 \phi_{n-1_\tau} + G_2 \phi_{n_\tau} + G_3 \phi_{n+1_\tau} \qquad \text{(B-2)}$$

where

$$G_1 = G_3 = \frac{1}{M_w}$$

$$G_2 = 1 - \frac{2}{M_w}$$

with $$M_w = \frac{(\Delta\eta)^2}{\Delta\tau}$$

Equations (B-1) and (B-2) apply only at intermediate stations in the web and in the flange. At the middle of the web,

$$\phi_{n_{\tau+\Delta\tau}} = G_2 \phi_{n_\tau} + 2 G_3 \phi_{n+1_\tau} \qquad \text{(B-3)}$$

and at the edge of the flange,

$$\phi_{n_{\tau+\Delta\tau}} = 2 F_1 \phi_{n-1_\tau} + F_2 \phi_{n_\tau} + F_4 \phi_{e_\tau} \qquad \text{(B-4)}$$

ϕ_{+o} and ϕ_{-o} are determined by expressing the derivatives in boundary condition (3) of Section III in finite difference form in the manner of Equation (A-4). This yields the following two relations,

$$-\left(\frac{\Delta\eta}{\Delta\xi}\right) \frac{1.5\,\phi_{+o} - 2\,\phi_1 + 0.5\,\phi_2}{1.5\,\phi_{-o} - 2\,\phi_{-1} + 0.5\,\phi_{-2}} = \frac{1}{2\gamma} \qquad \text{(B-5)}$$

and

$$\frac{1}{\Delta\eta}\left(1.5\,\phi_{-o} - 2\,\phi_{-1} + 0.5\,\phi_{-2}\right) = \lambda_j\left(\phi_{+o} - \phi_{-o}\right) \tag{B-6}$$

which may be solved simultaneously to yield

$$\phi_{-o_\tau} = C_{-1}\,\phi_{-1_\tau} + C_{-2}\,\phi_{-2_\tau} + C_1\,\phi_{1_\tau} + C_2\,\phi_{2_\tau} \tag{B-7}$$

$$\phi_{+o_\tau} = D_{-1}\,\phi_{-1_\tau} + D_{-2}\,\phi_{-2_\tau} + D_1\,\phi_{1_\tau} + D_2\,\phi_{2_\tau} \tag{B-8}$$

where

$$C_{-1} = \frac{4N}{1+3N}$$

$$C_{-2} = -\frac{N}{1+3N}$$

$$C_1 = \frac{4}{3(1+3N)}$$

$$C_2 = -\frac{1}{3(1+3N)}$$

$$D_{-1} = \frac{2}{3\gamma}\,\frac{\Delta\xi}{\Delta\eta}\,\frac{1}{1+3N}$$

$$D_{-2} = -\frac{1}{6\gamma}\,\frac{\Delta\xi}{\Delta\eta}\,\frac{1}{1+3N}$$

$$D_1 = \left(4 + \frac{6}{\lambda_j\,\Delta\eta}\right)\frac{1}{3(1+3N)}$$

$$D_2 = -\left(1 + \frac{1.5}{\lambda_j\,\Delta\eta}\right)\frac{1}{3(1+3N)}$$

with $$N = \frac{0.5}{\lambda_j \Delta\eta} + \frac{1}{6r}\frac{\Delta\xi}{\Delta\eta}$$

The problem of convergence must be considered here as it was in the case of the plate. The stability criteria will be the same as for the plate, that is,

$$F_2 \geqslant 0, \qquad G_2 \geqslant 0$$

yielding

$$M_f \geqslant 2 + \lambda(\Delta\xi)^2, \qquad M_w \geqslant 2$$

where again it is desirable that the M's be substantially greater than the values indicated by the equality.

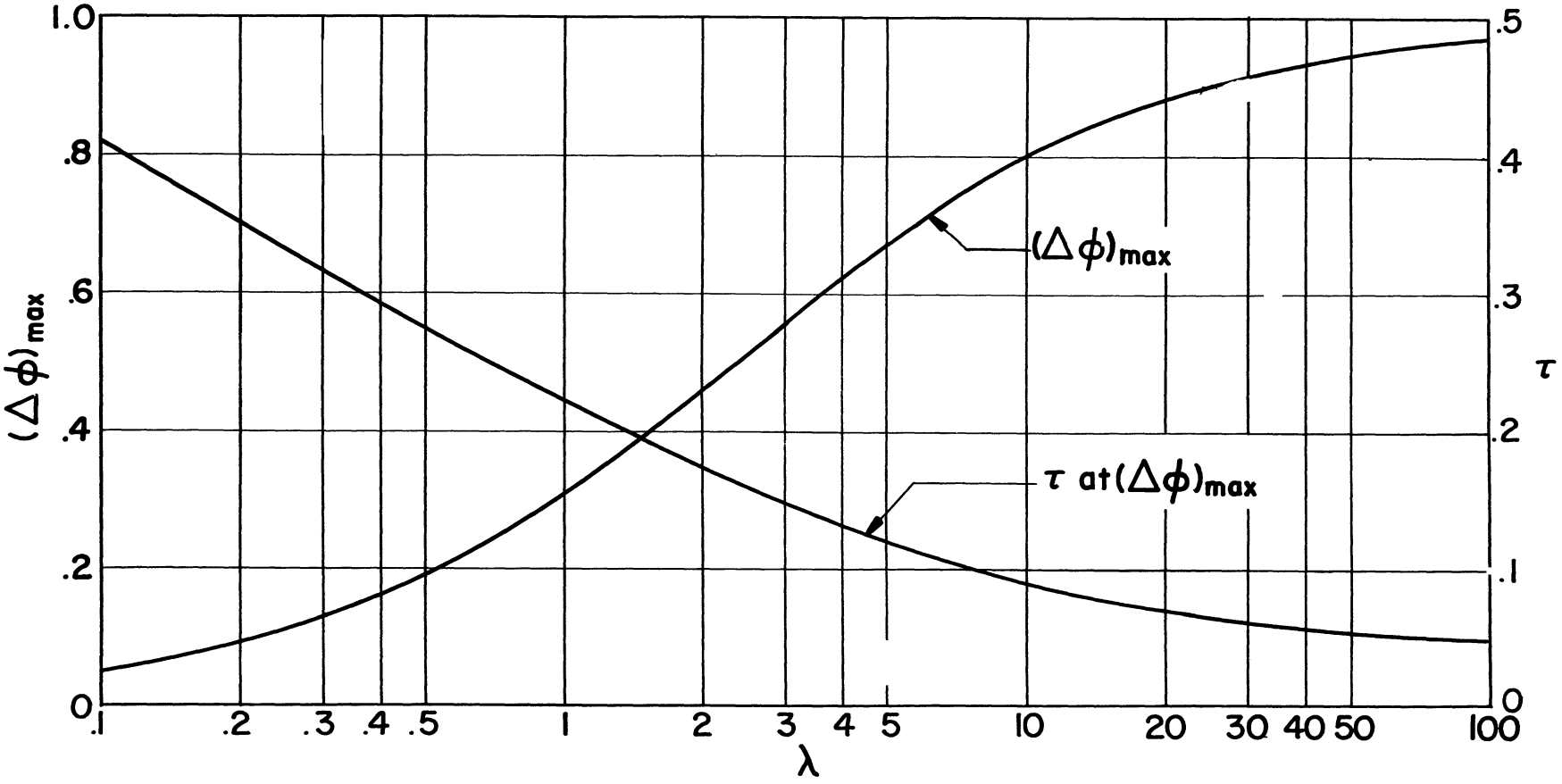

Fig. 1 - Maximum temperature differential across the surfaces of a flat plate subjected to a sudden change in environment temperature.

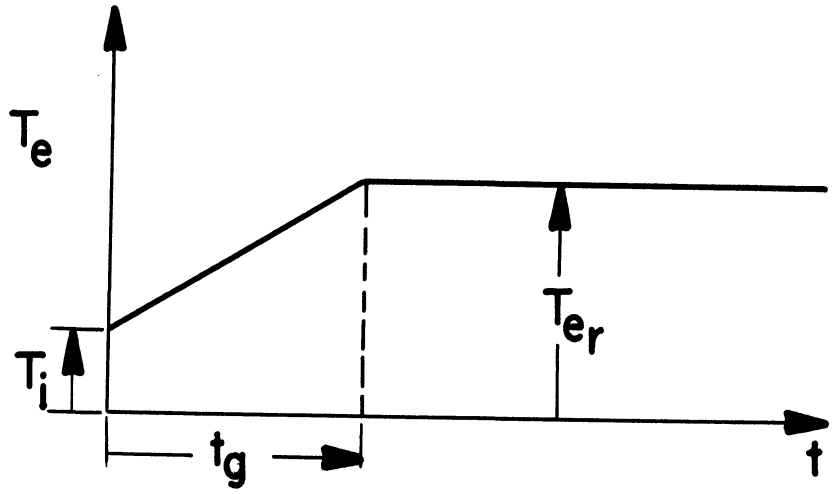

(a) Dimensional form.

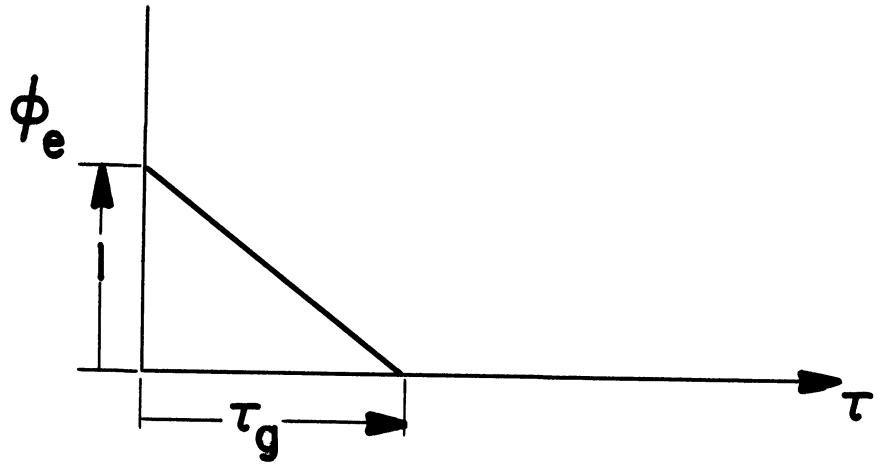

(b) Non-dimensional form.

Fig. 2 - Assumed variation of environment temperature with time.

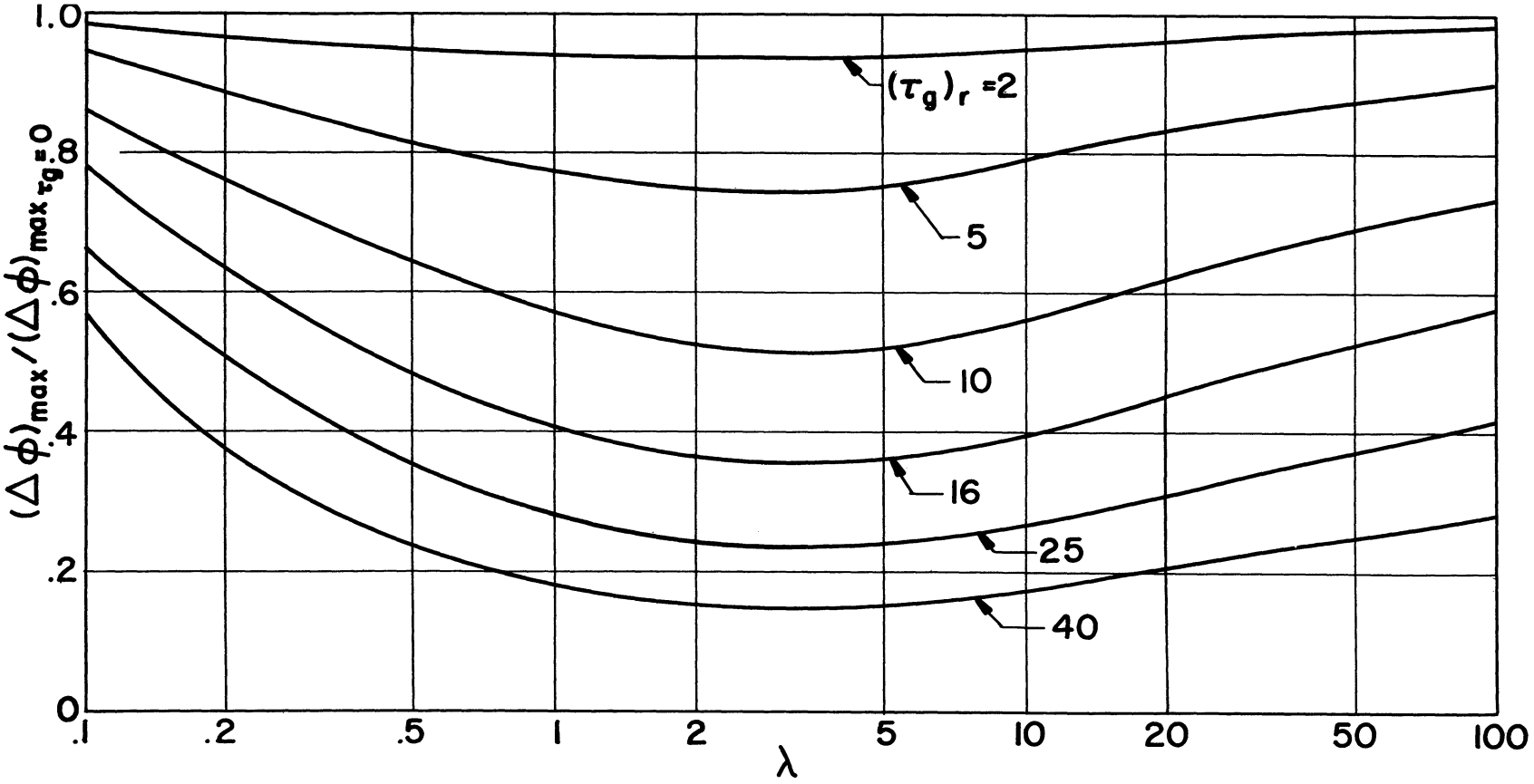

Fig. 3 - Effect of gradient time on the maximum temperature differential across the surfaces of a flat plate.

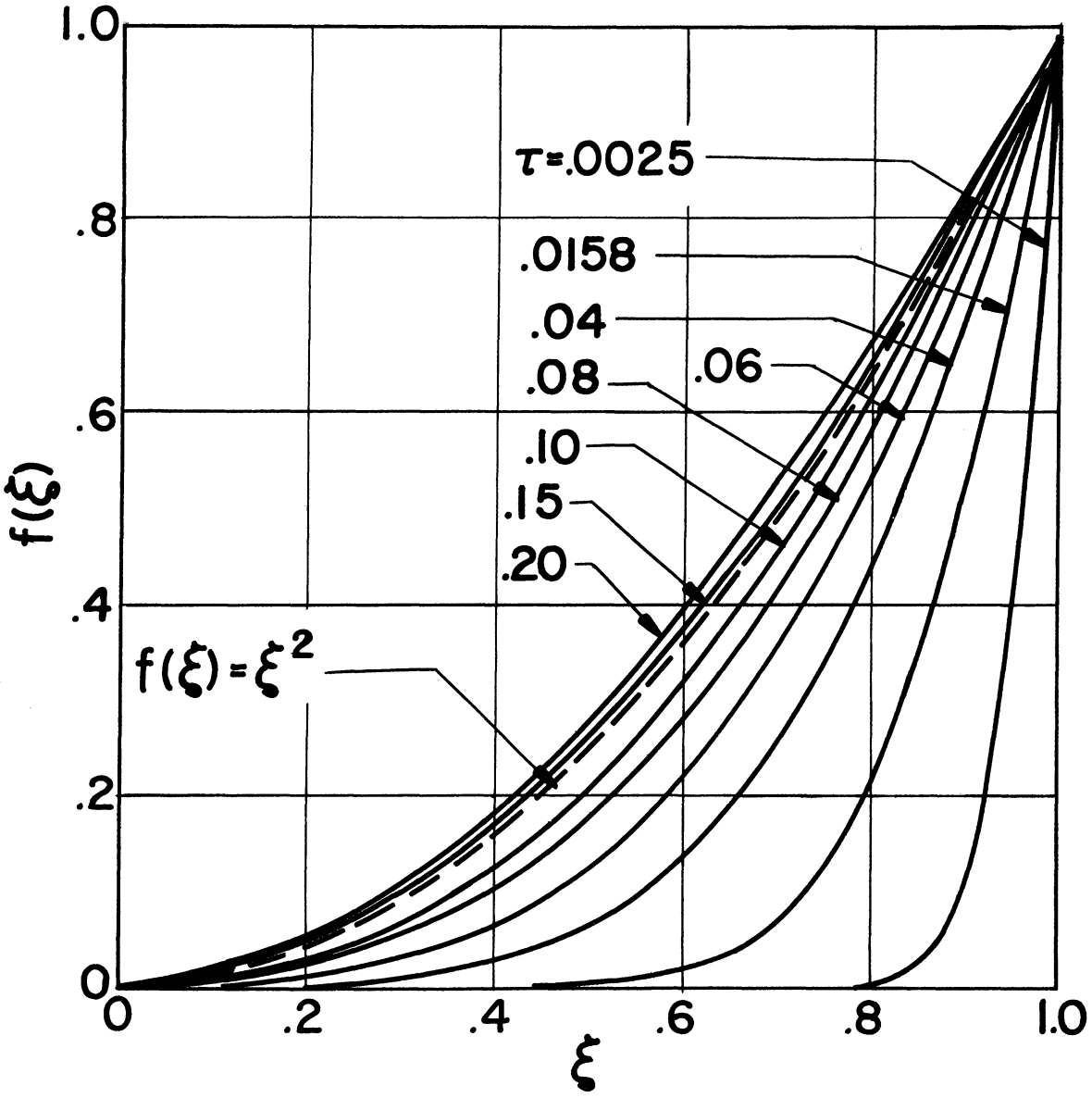

Fig. 4 - Change of temperature distribution with time during heating of a flat plate. $\lambda = 20$.

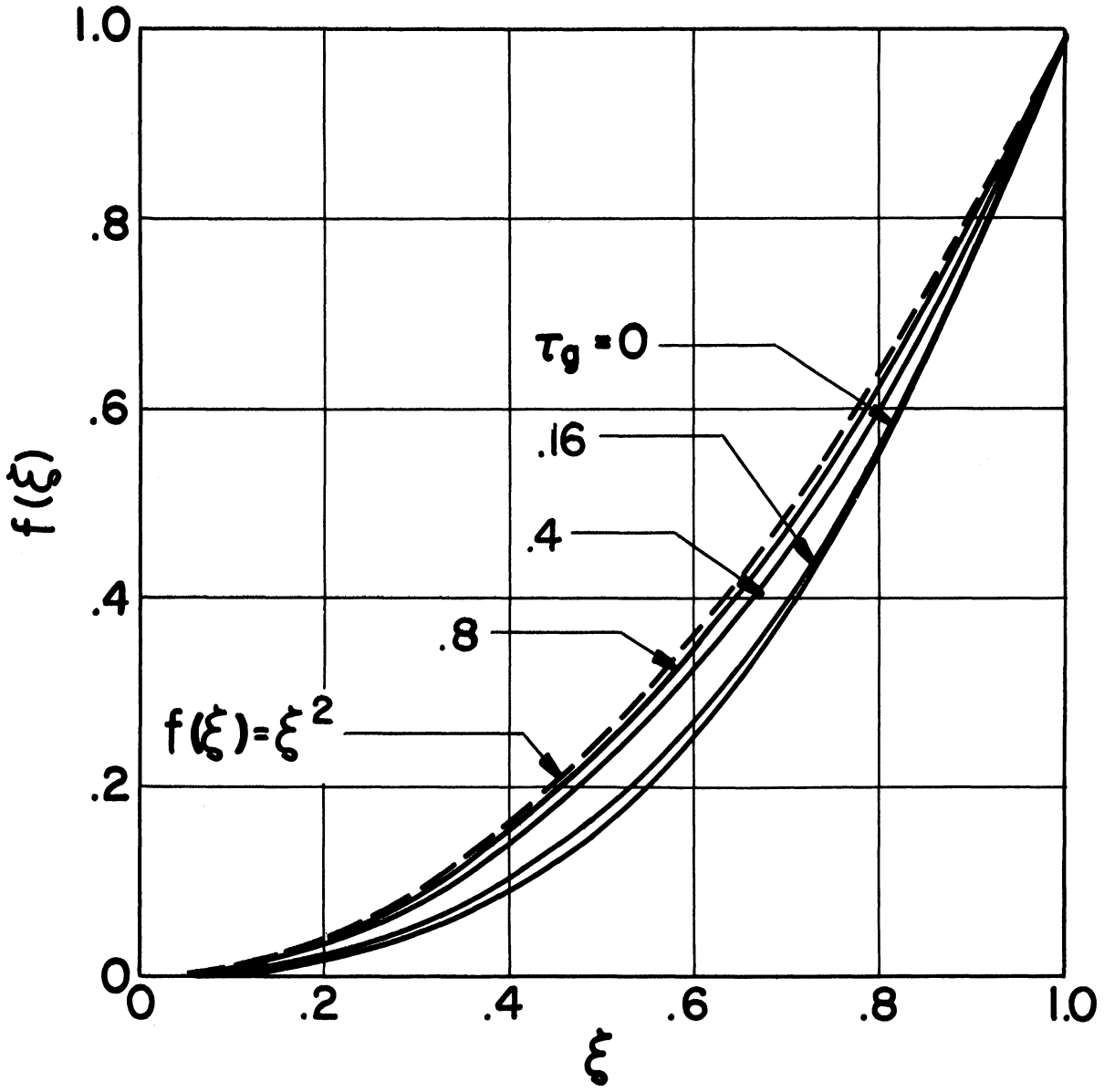

Fig. 5 - Effect of gradient time on temperature distribution at time of maximum temperature differential in a flat plate. $\lambda = 20$.

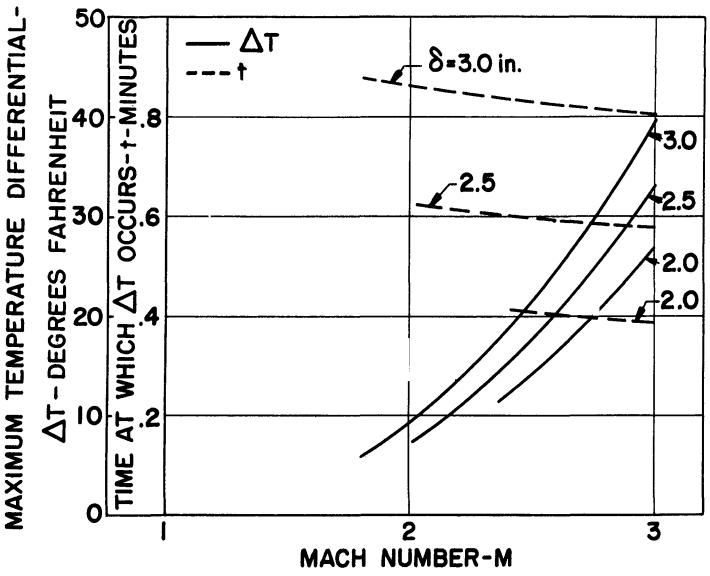

(a) Aluminum alloy.

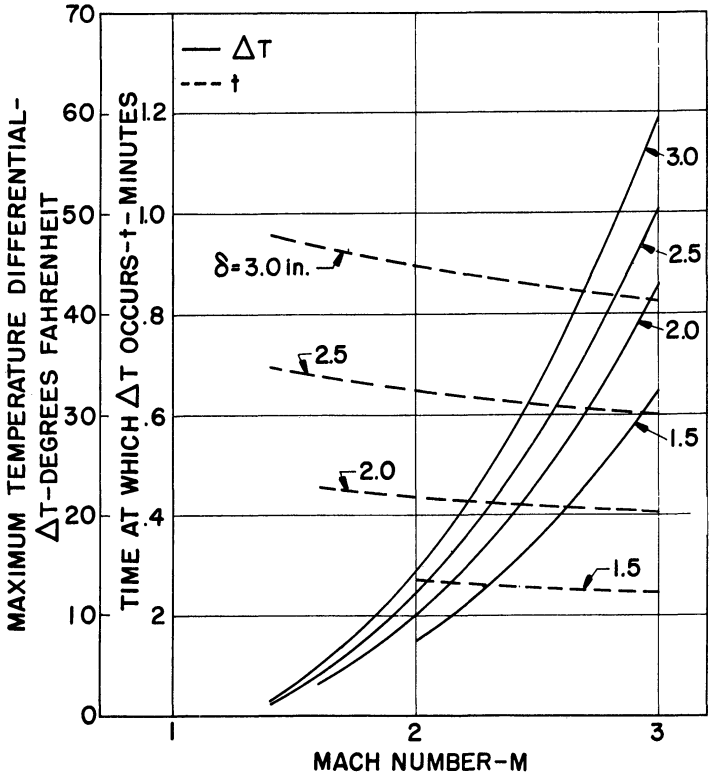

(b) Magnesium alloy.

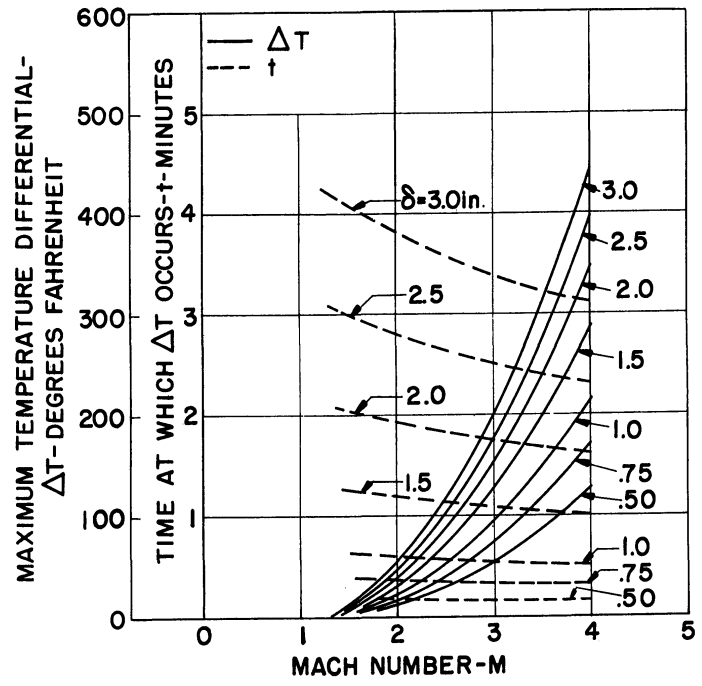

(c) Titanium alloy.

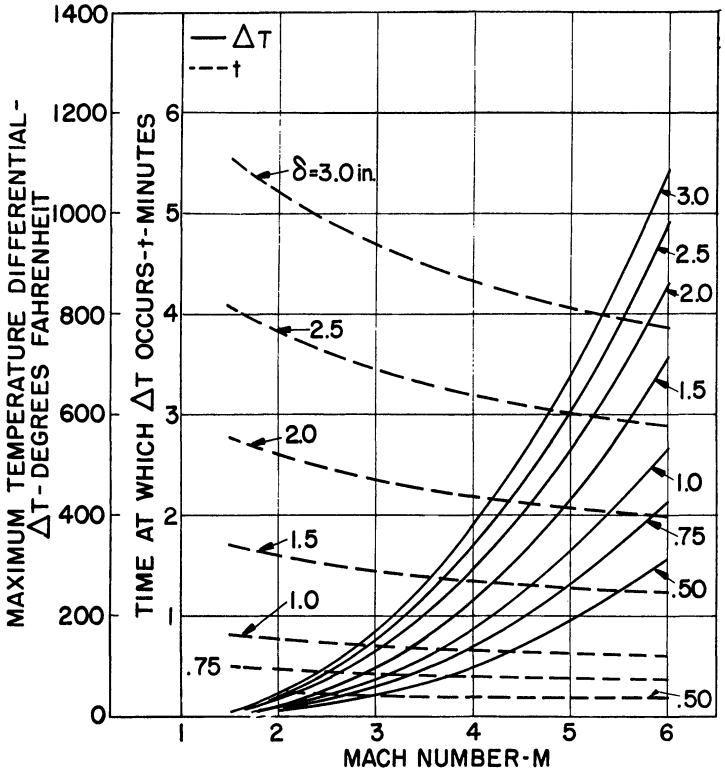

(d) Stainless steel.

Fig. 6 - Maximum temperature differential due to aerodynamic heating of a flat plate.

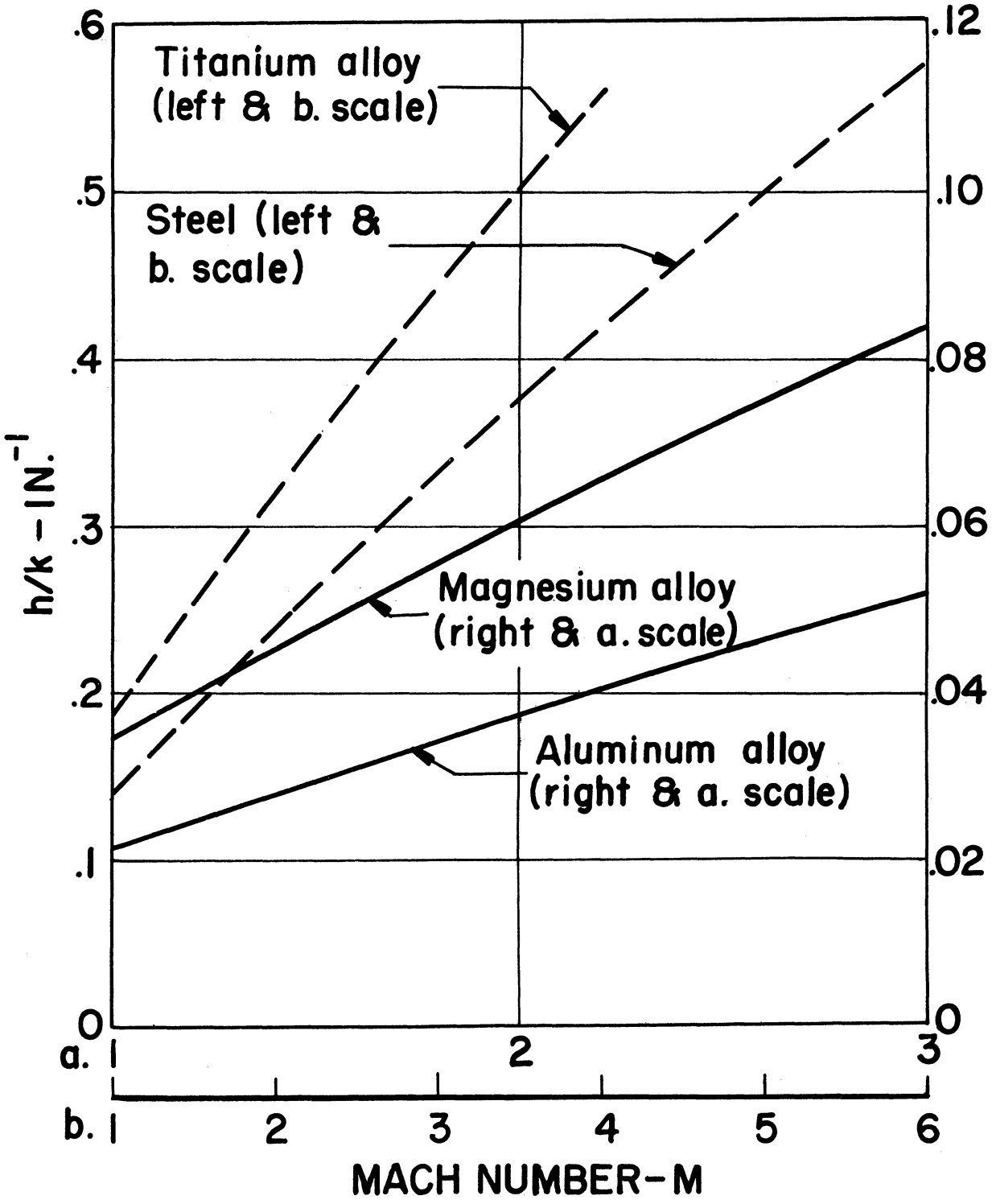

Fig. 7 - Ratio of heat transfer coefficient to thermal conductivity.

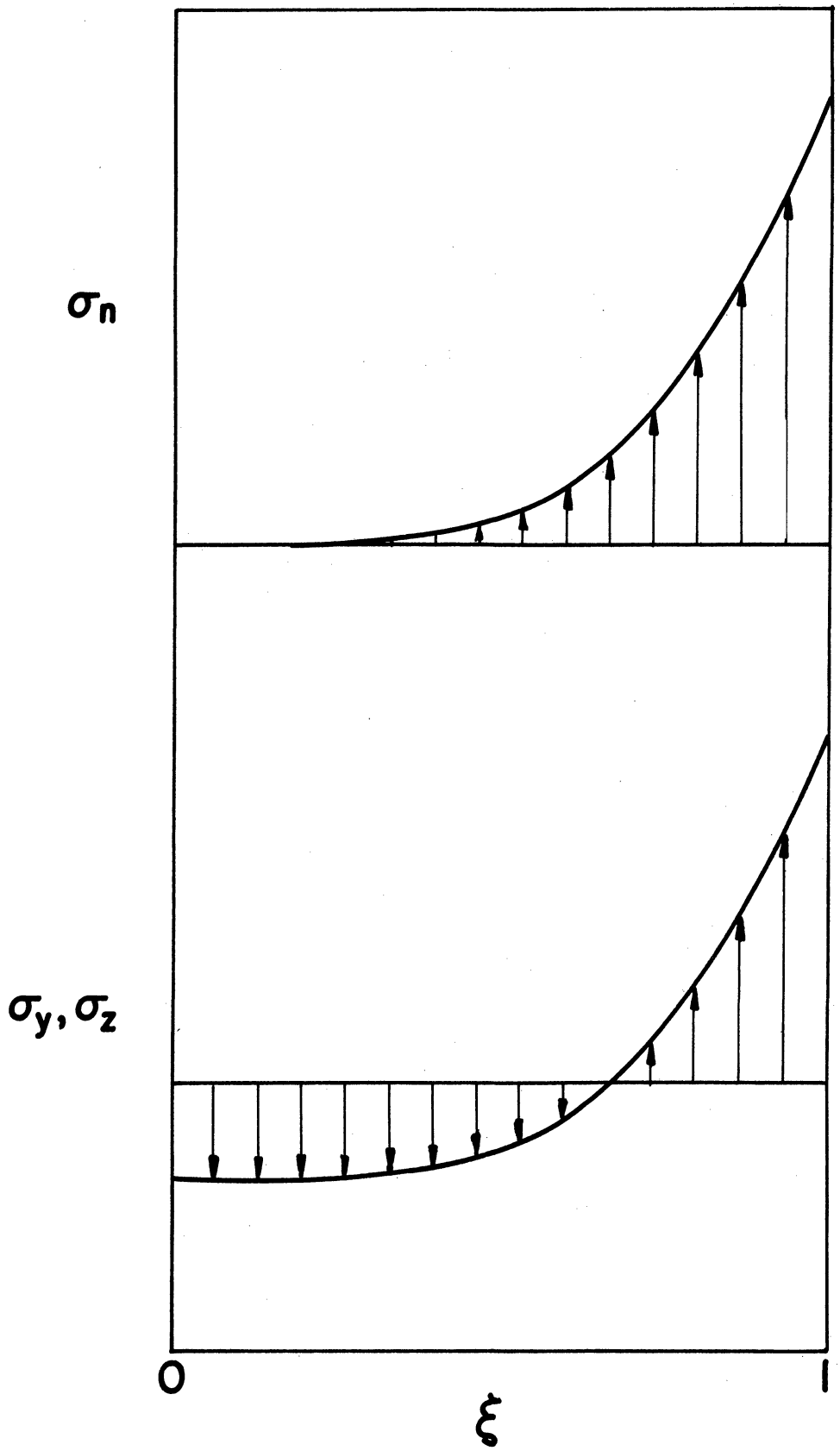

Fig. 8 - Thermal stress distribution in a flat plate with edges restrained against bending.

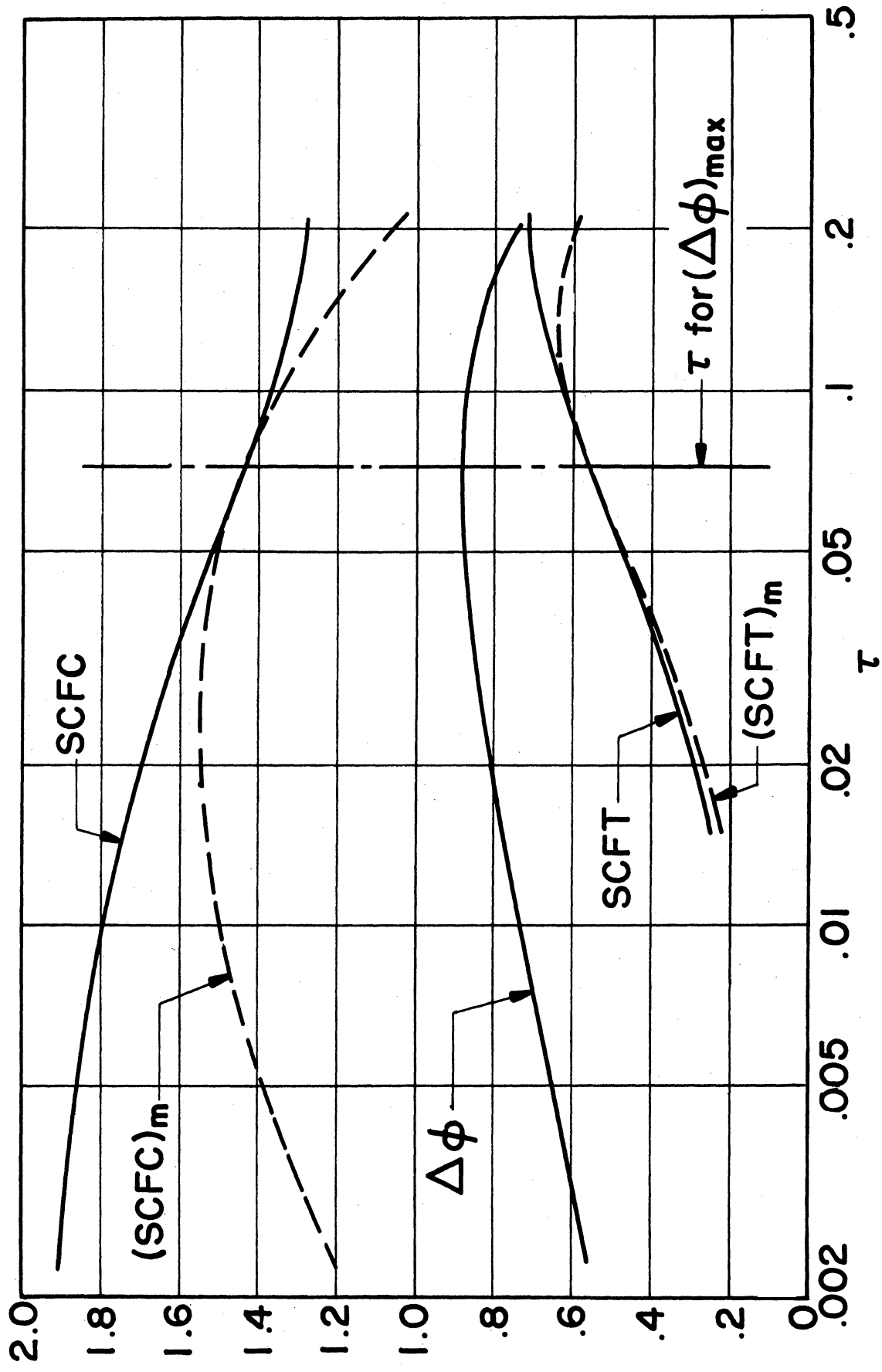

Fig. 9 - Variation of stress correction factors with time during heating of a flat plate. $\lambda = 20$. $\tau_g = 0$.

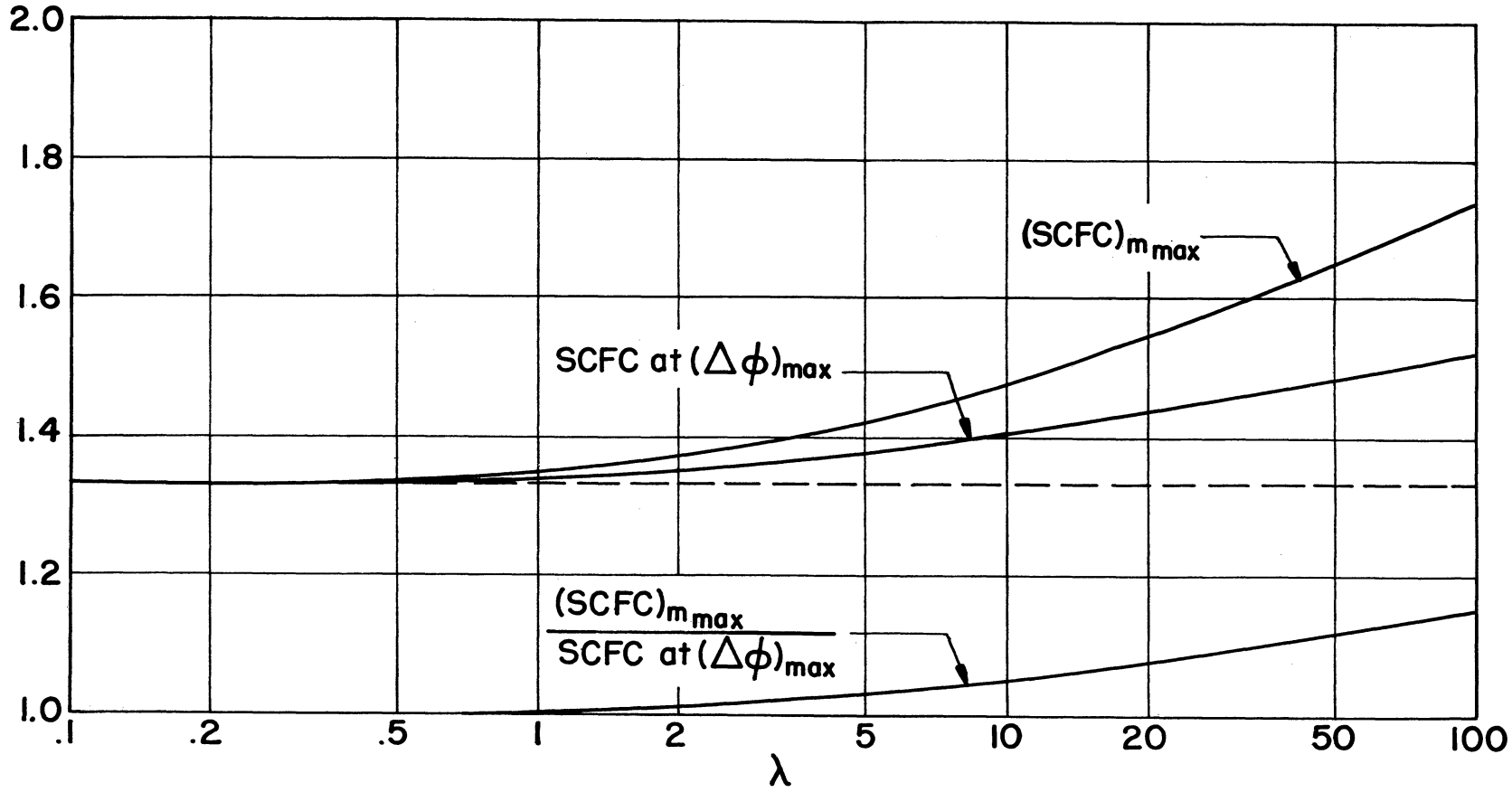

Fig. 10 - Variation of stress correction factors with λ. Flat plate. $\tau_g = 0$.

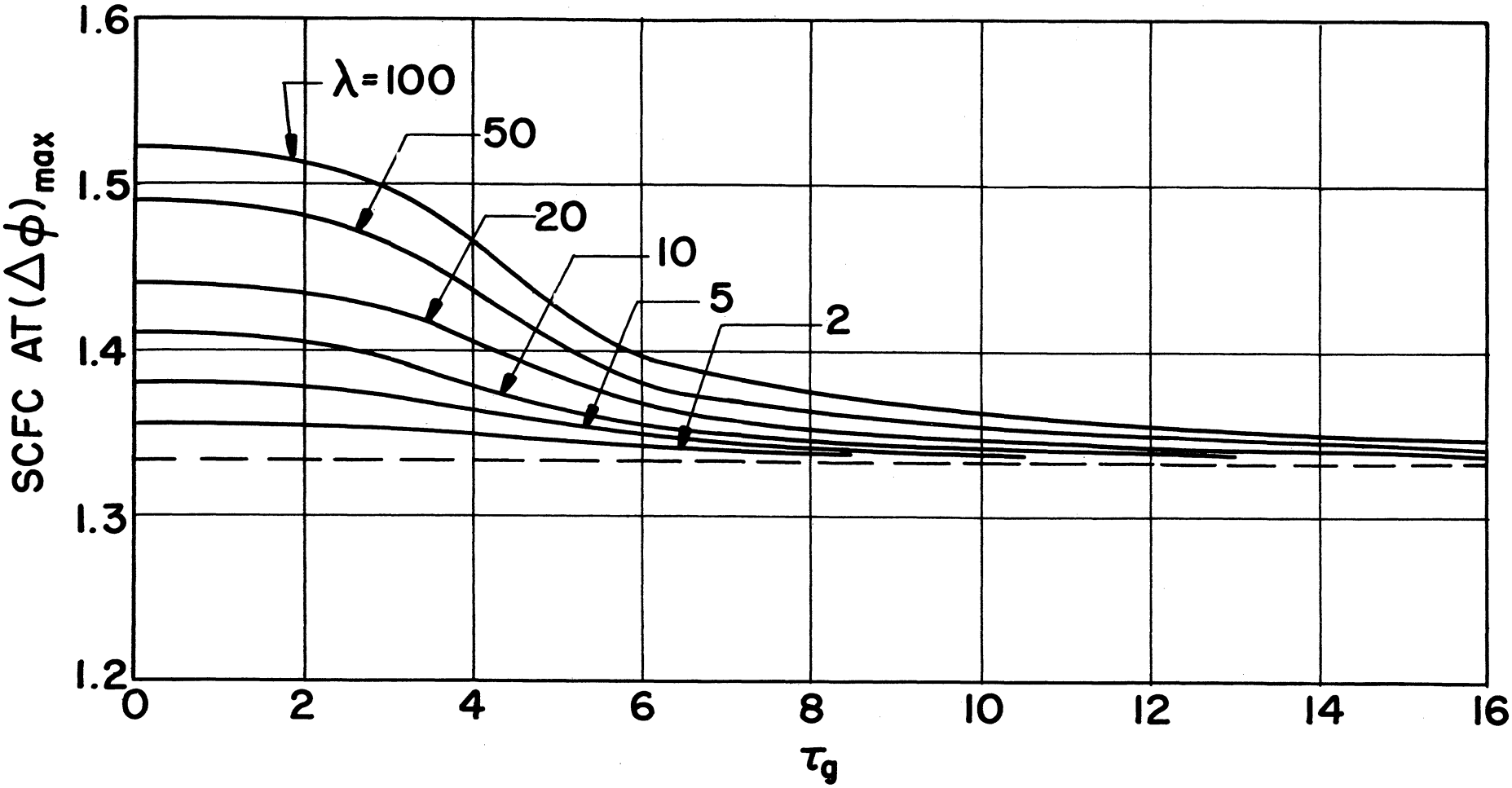

Fig. 11 - Effect of gradient time on the stress correction factor at maximum temperature differential in a flat plate.

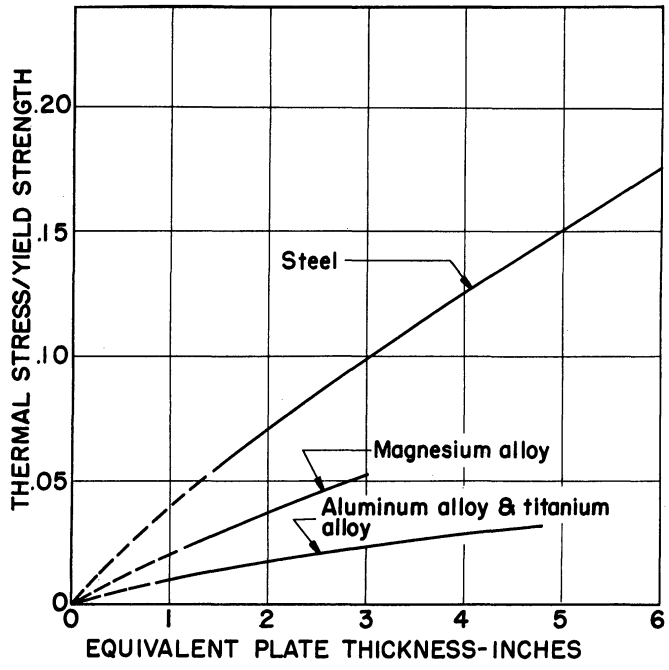

(a) M = 2.0

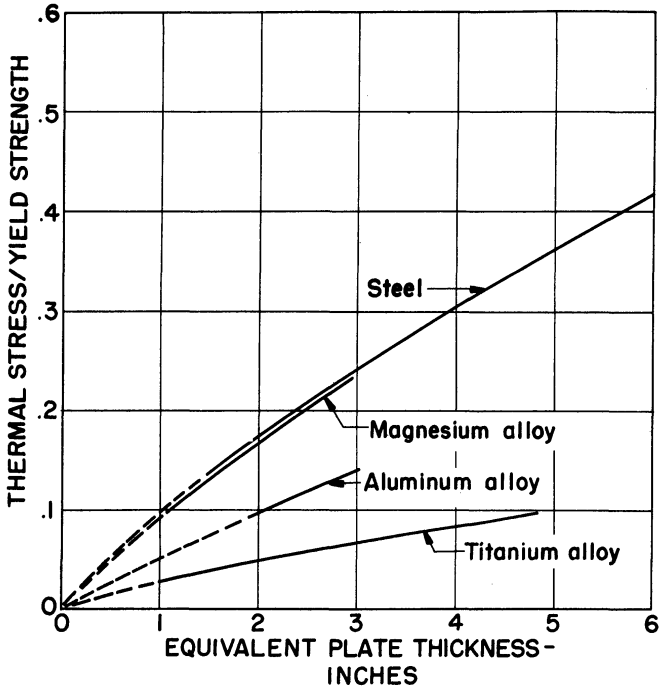

(b) M = 2.5

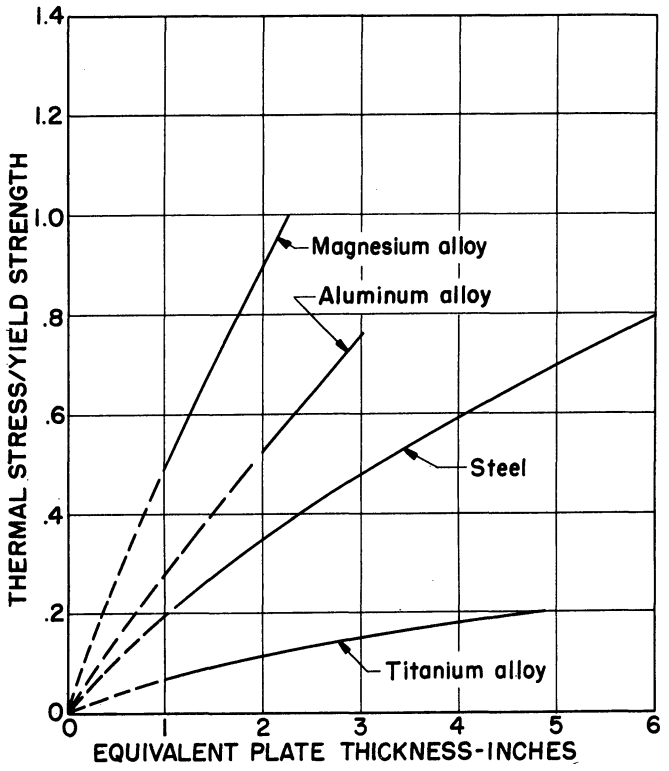

(c) M = 3.0

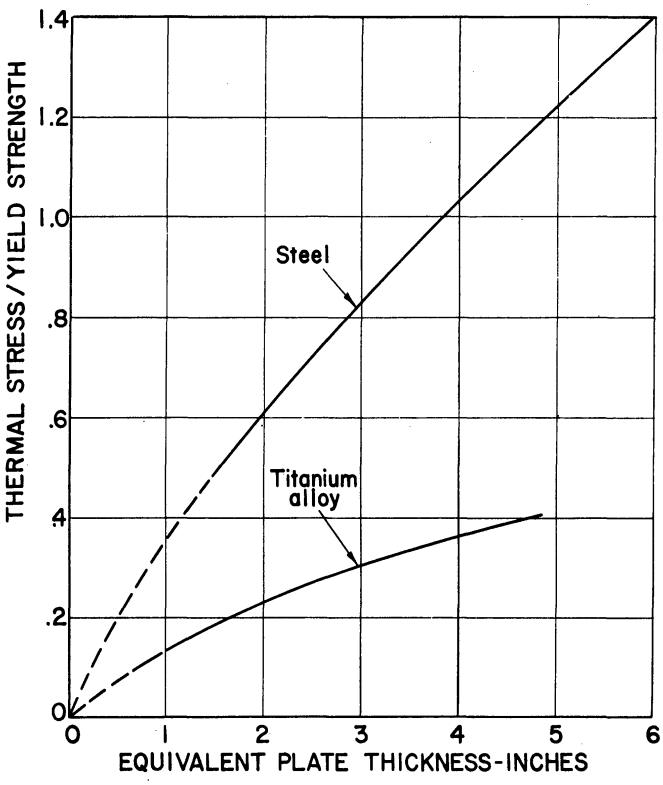

(d) M = 3.5

Fig. 12 - Ratio of thermal stress to yield strength for aerodynamic heating of a flat plate. Linear temperature distribution.

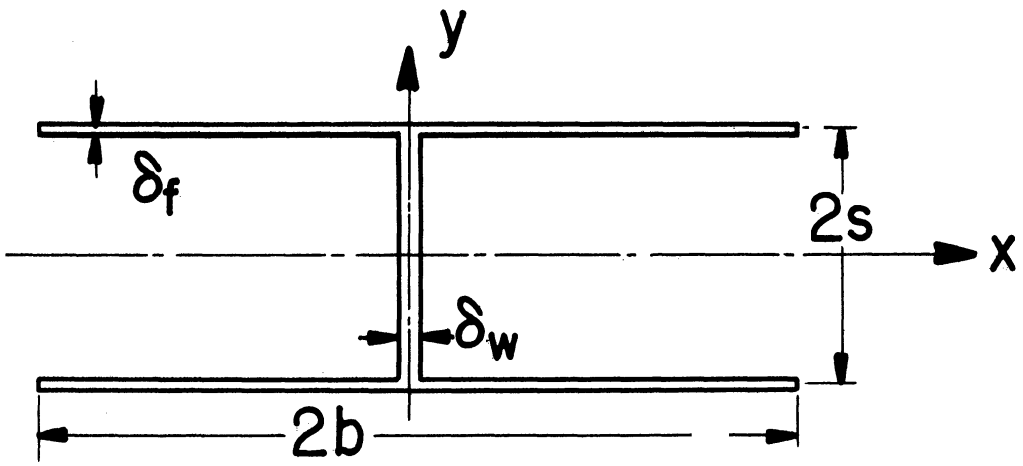

Fig. 13 - Cross-section of I-beam.

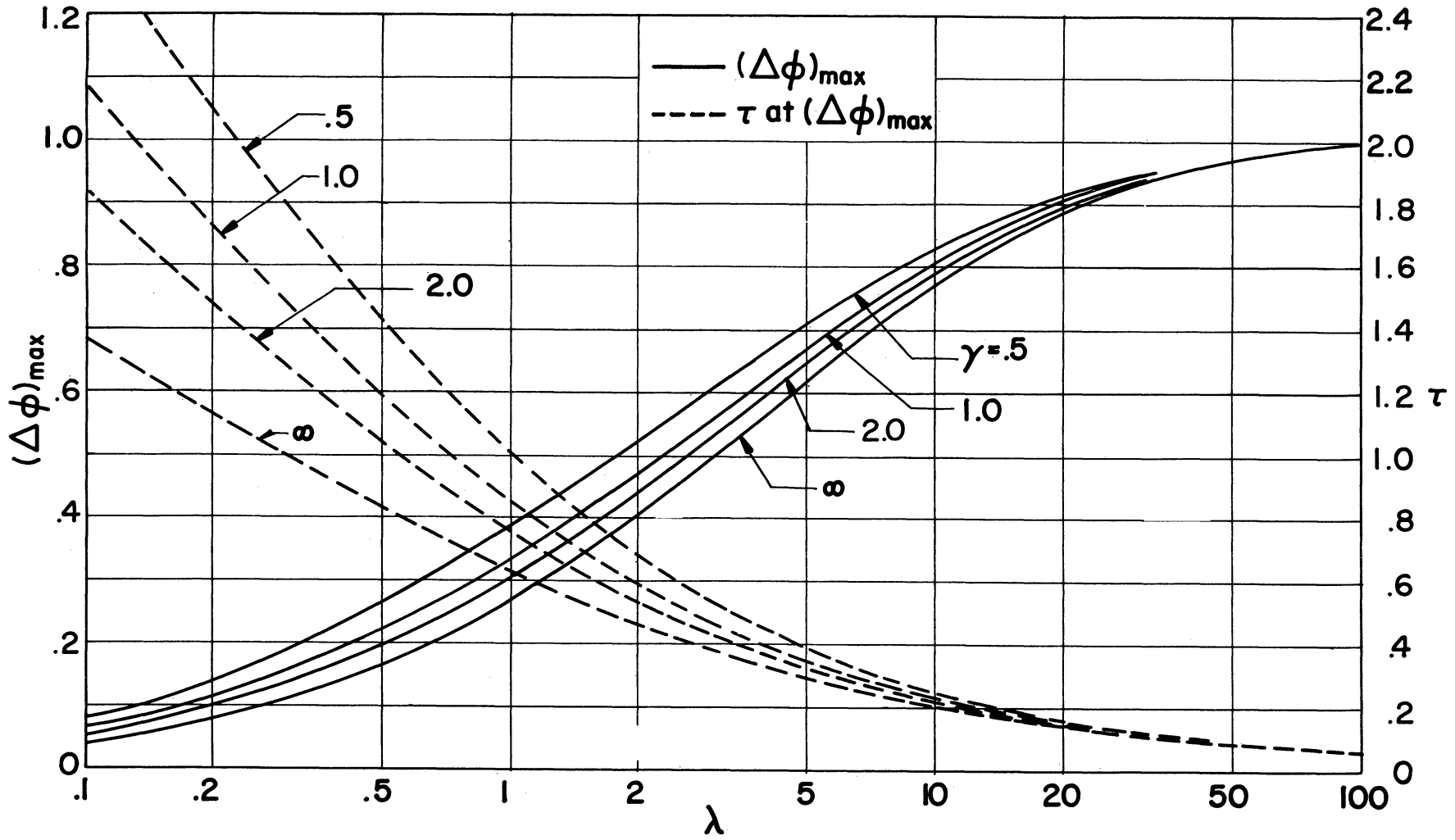

Fig. 14 - Maximum temperature differential in a wide-flanged I-beam subjected to a sudden change in environment temperature.

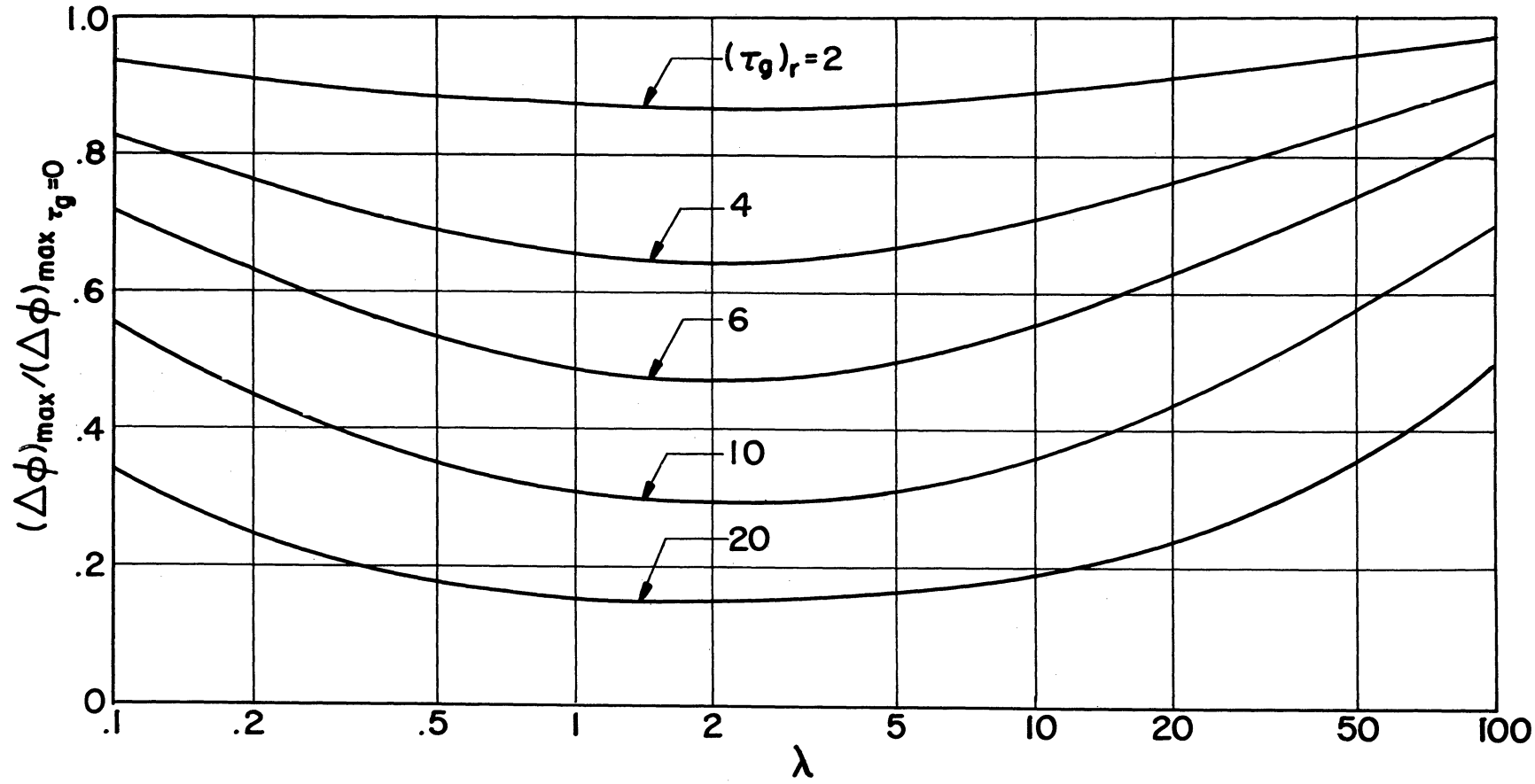

Fig. 15 - Effect of gradient time on the maximum temperature differential in a wide-flanged I-beam.

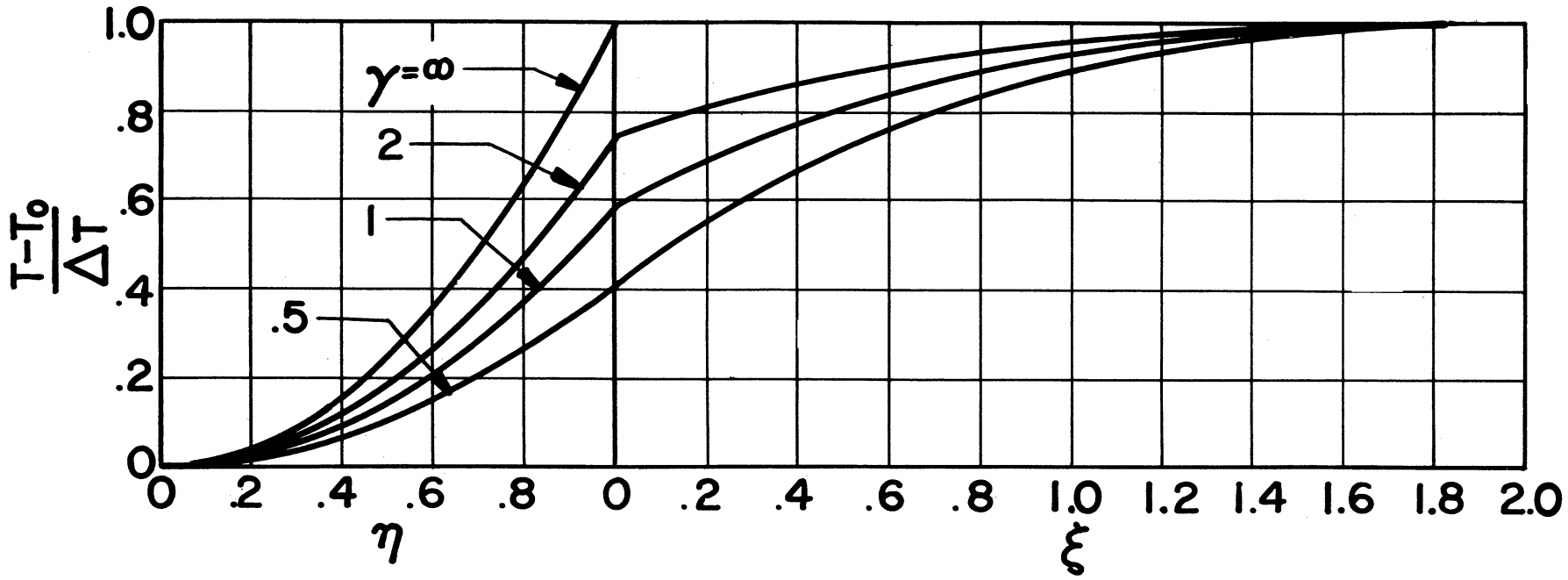

Fig. 16 - Effect of γ on temperature distribution at time of maximum temperature differential in a wide-flanged I-beam. $\lambda = 1$. $\tau_g = 0$.

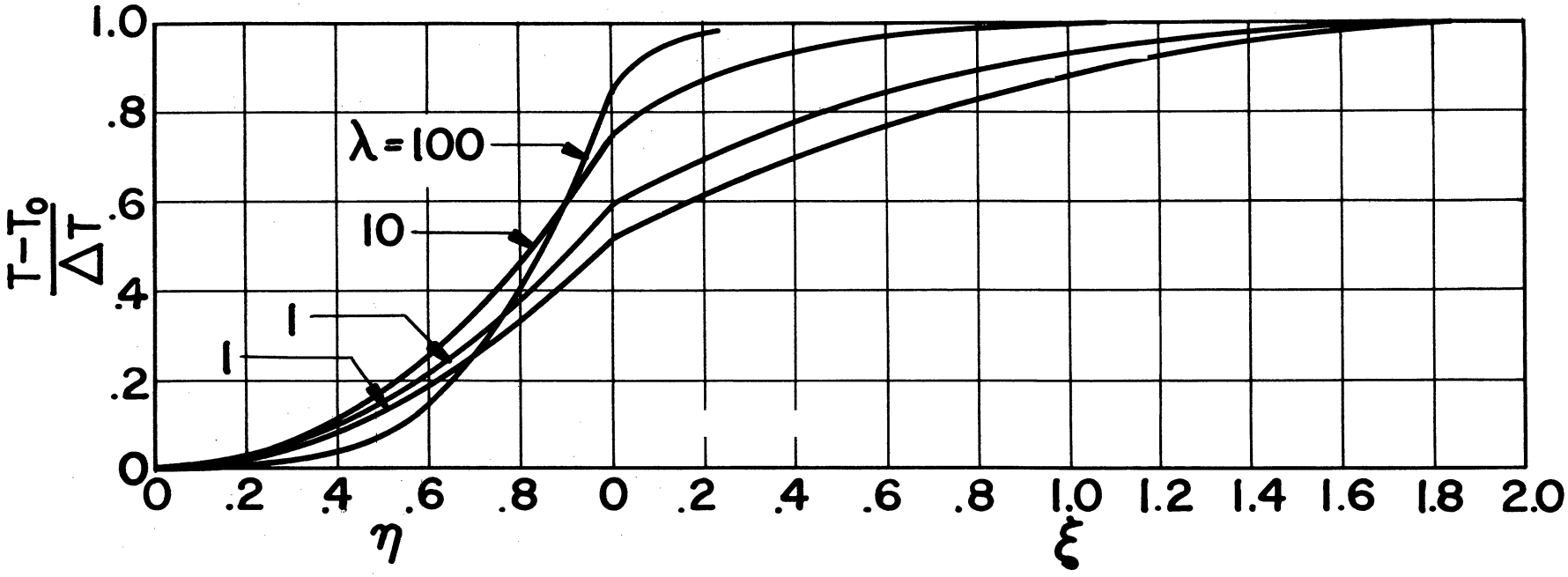

Fig. 17 - Effect of λ on temperature distribution at time of maximum temperature differential in a wide-flanged I-beam. $\gamma = 1$. $\tau_g = 0$.

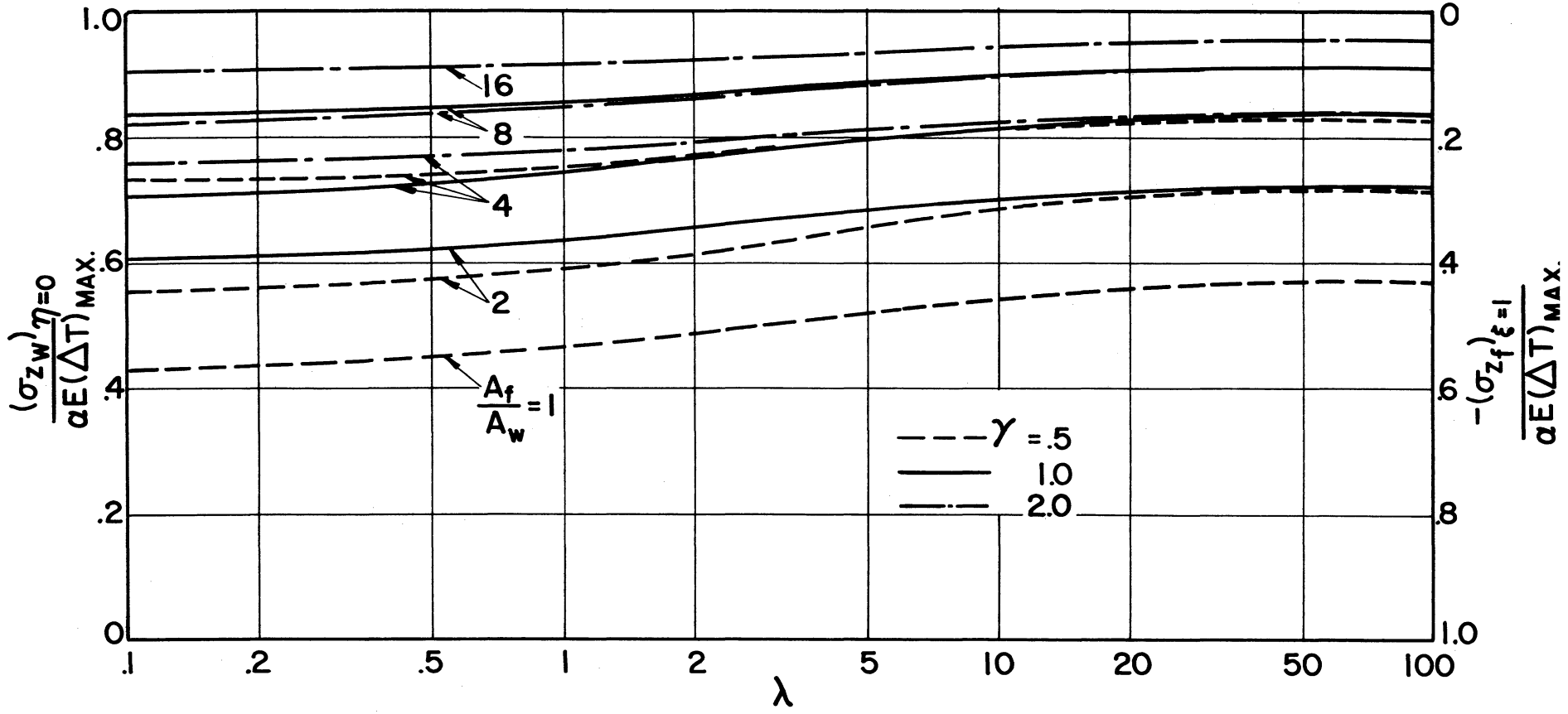

Fig. 18 - Effect of λ on relative proportions of maximum tensile and compressive stresses in stress range of wide-flanged I-beam.

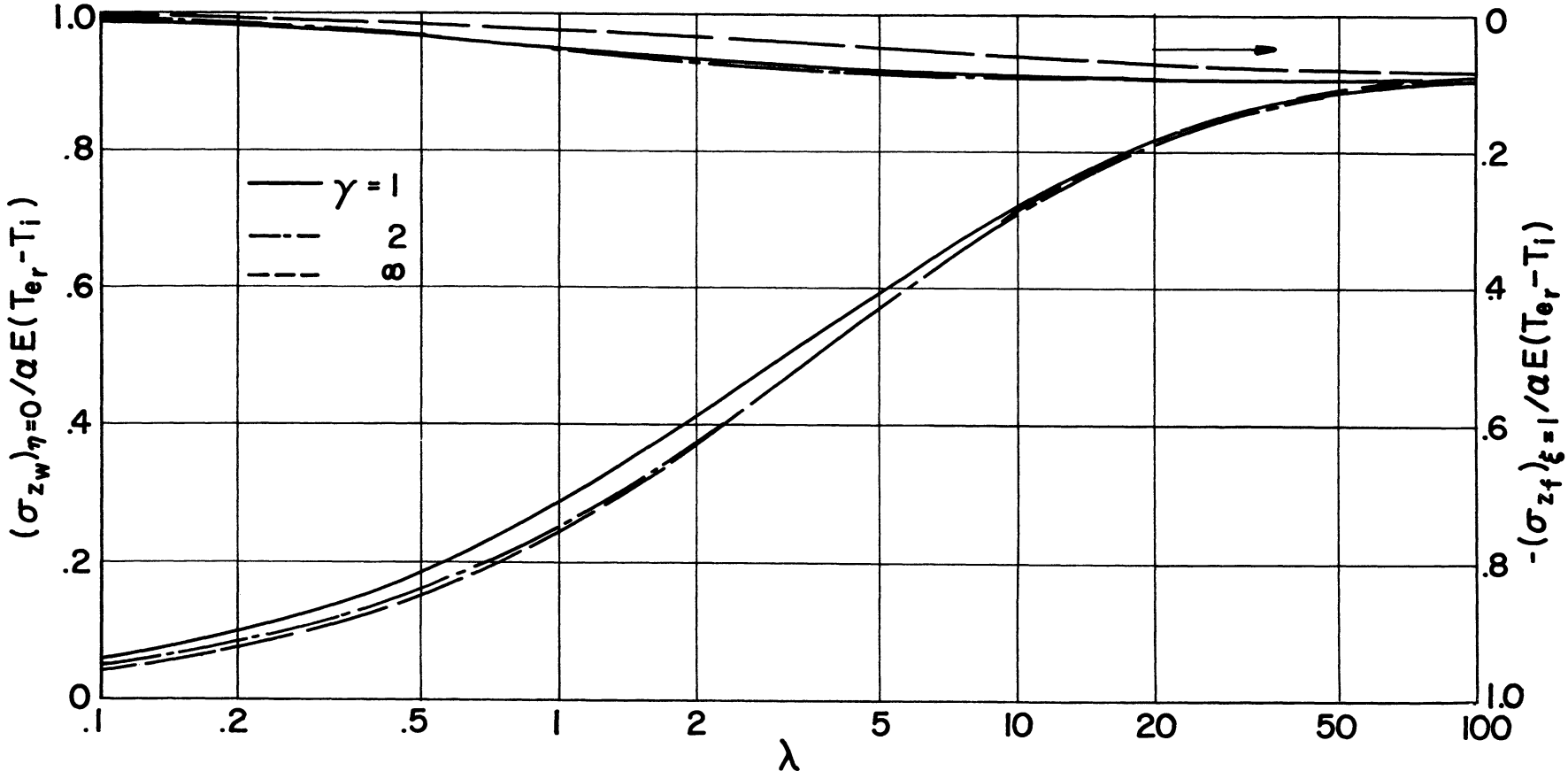

Fig. 19 - Effect of λ on maximum tensile and compressive stresses in wide-flanged I-beam. $A_f/A_w = 8$.

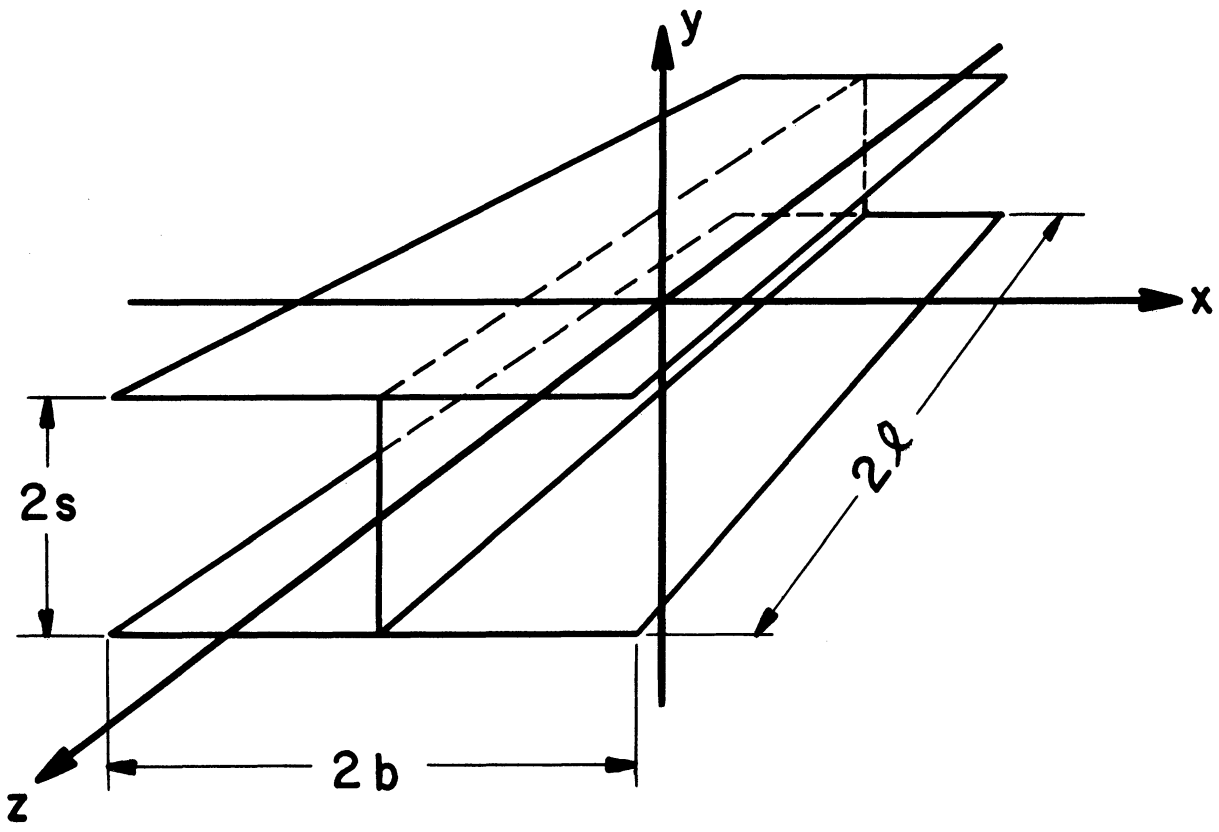

Fig. 20 - Coordinate axes and dimensions of wide-flanged I-beam.

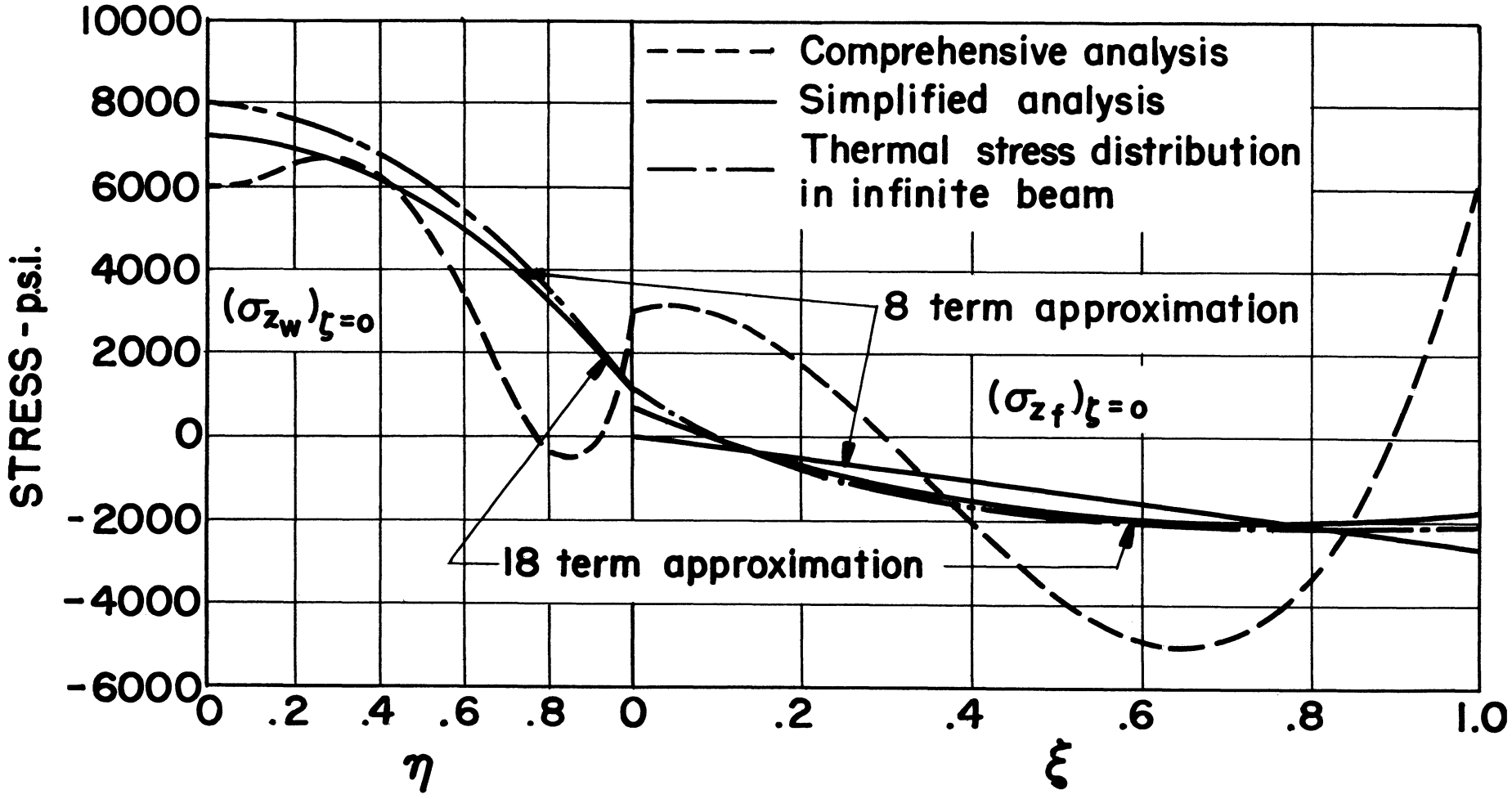

Fig. 21 - Distribution of logitudinal stress in middle section of I-beam.

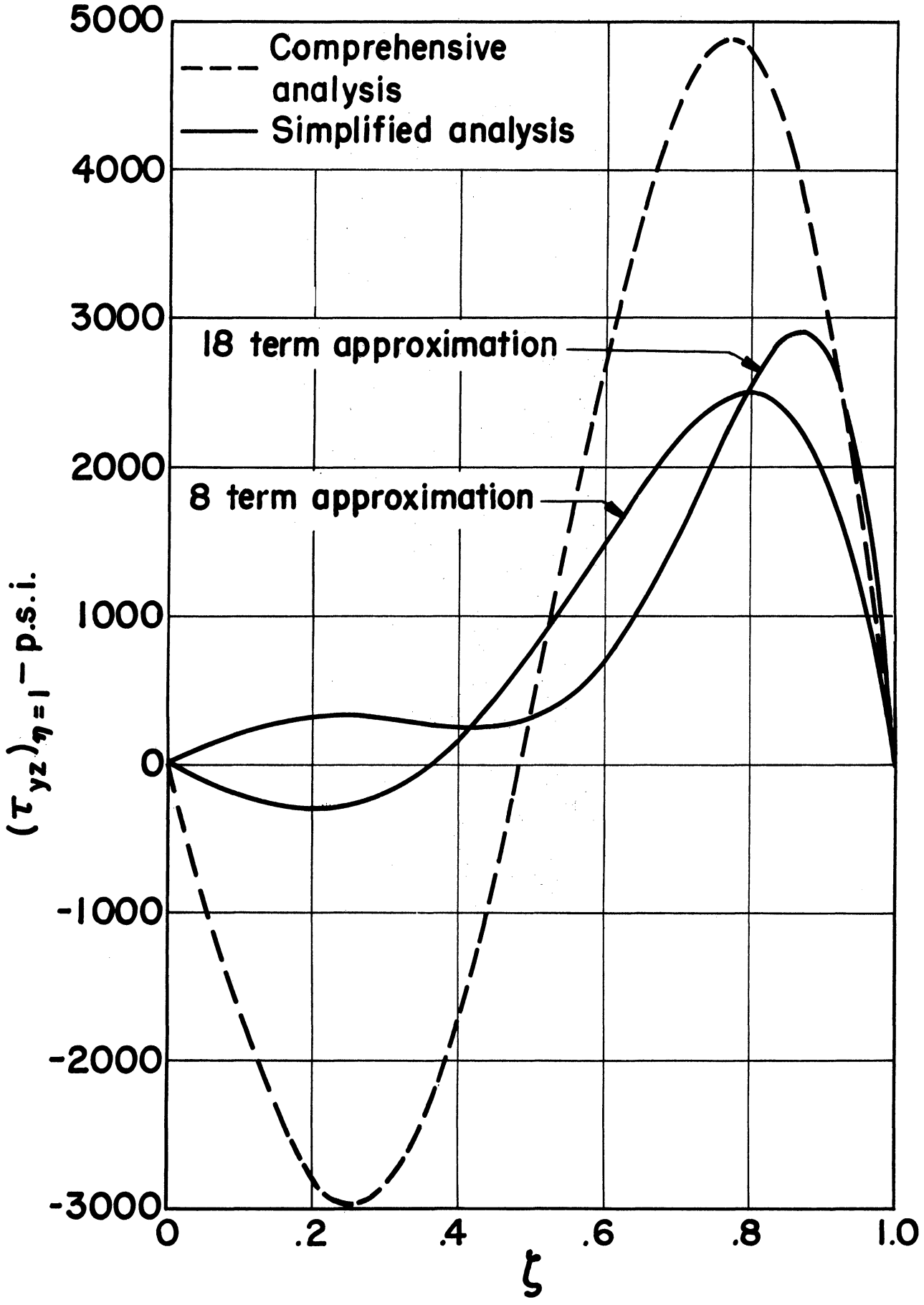

Fig. 22 - Distribution of shear stress in web of I-beam along joint with flange.

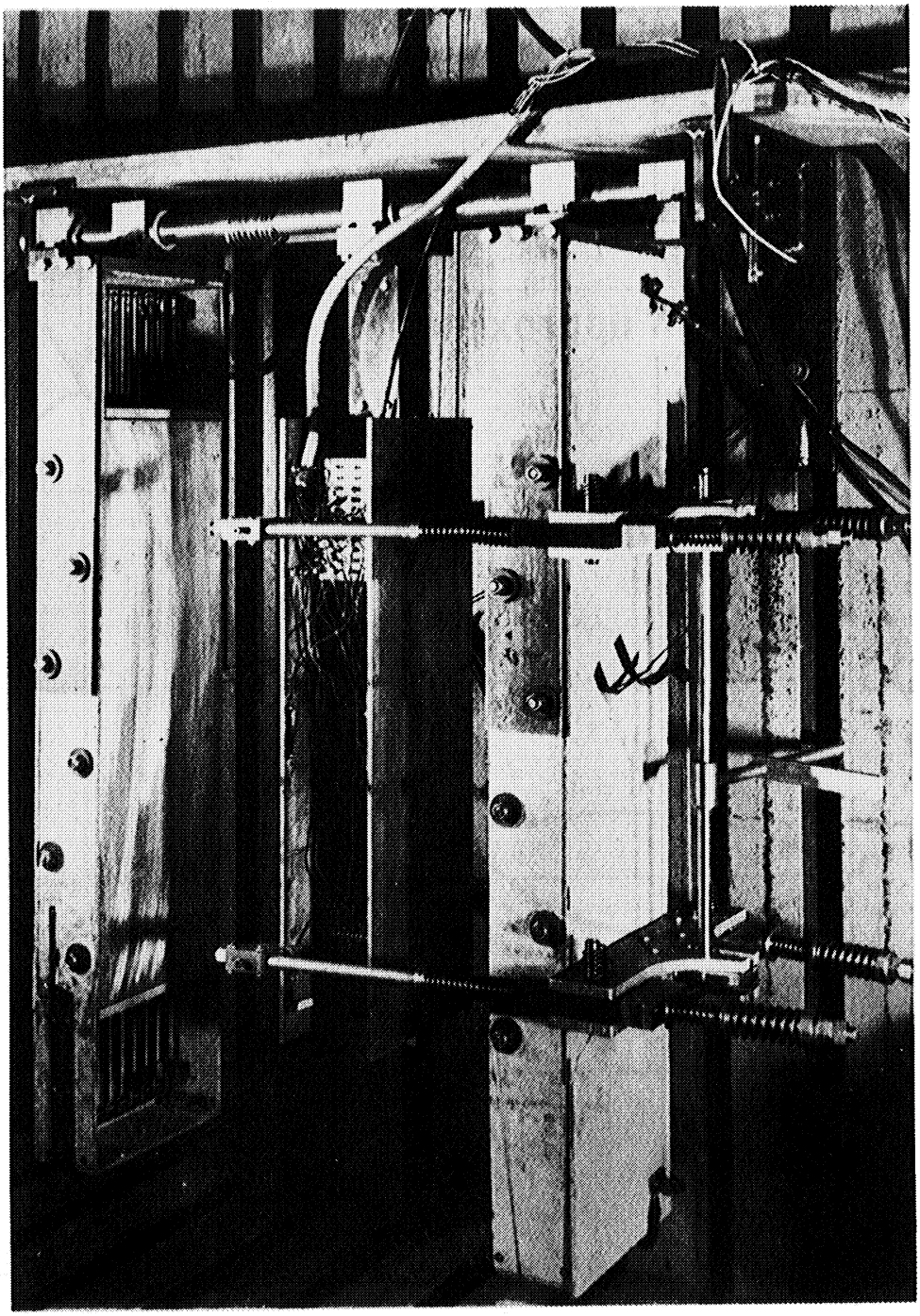

Fig. 23 - Experimental set-up for I-beam heating and thermal stress measurements.

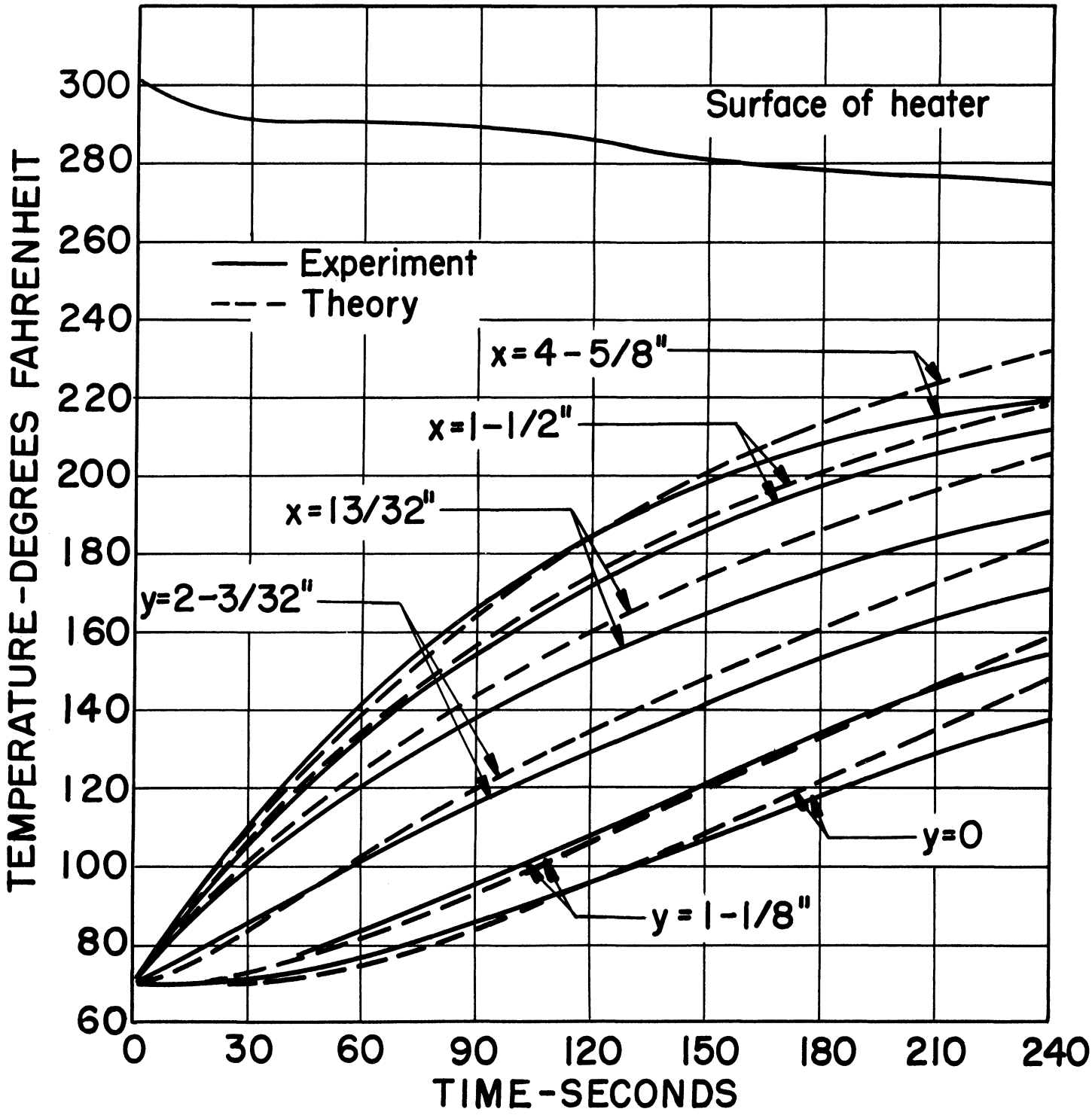

Fig. 24 - Temperature variation with time at gage locations in middle section of I-beam.

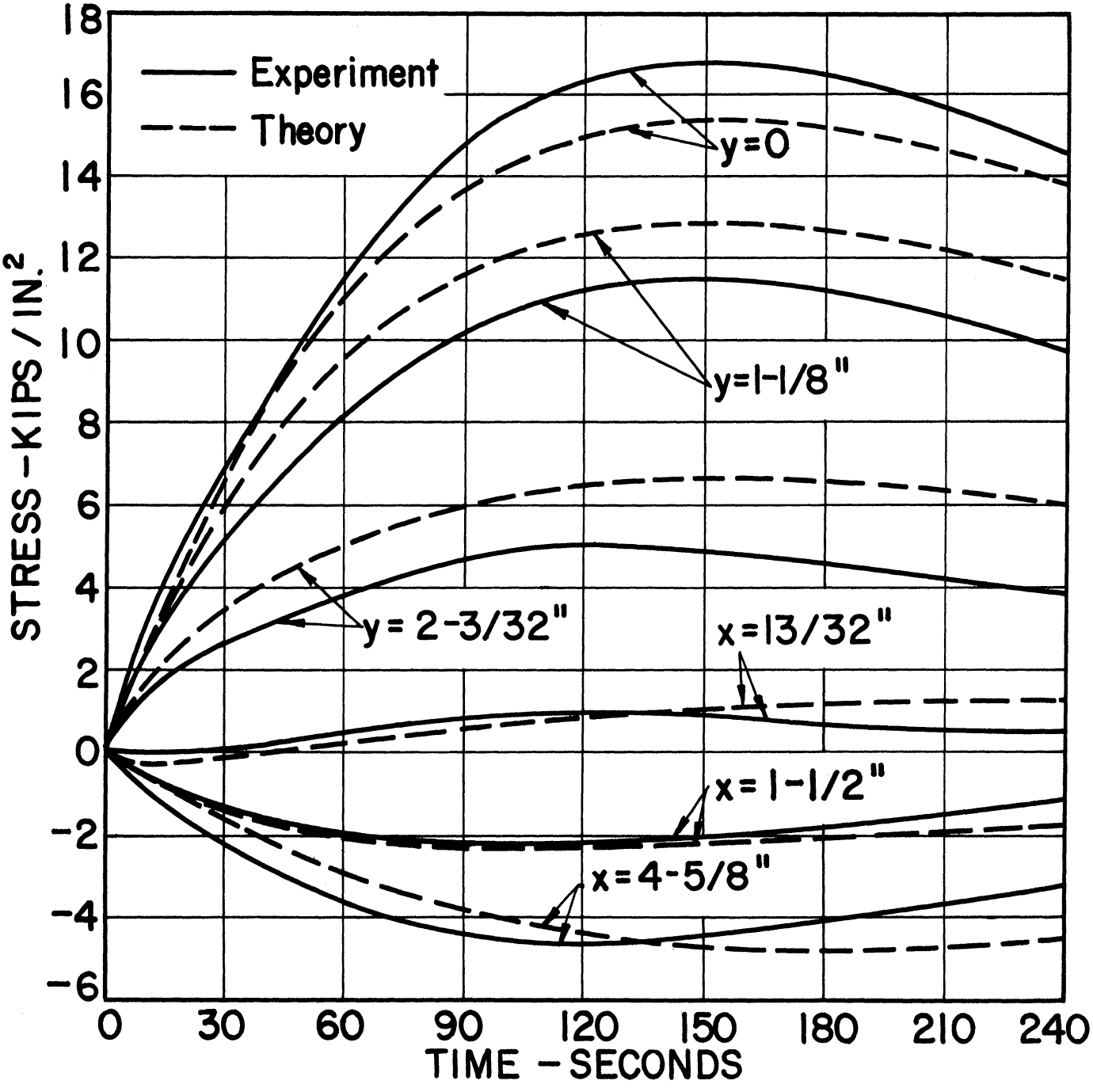

Fig. 25 - Stress variation with time at gage locations in middle section of I-beam.

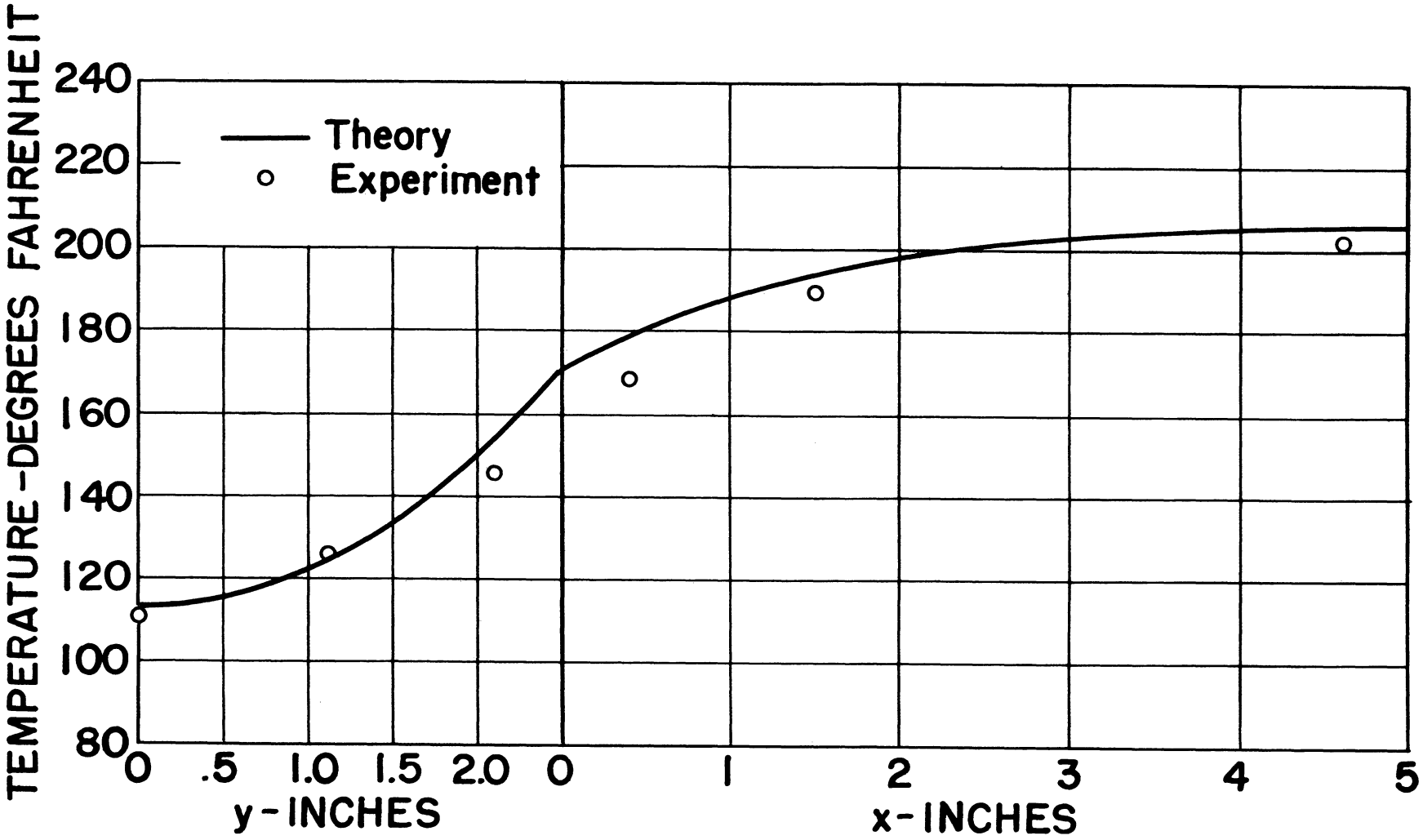

Fig. 26 - Distribution of temperature in middle section of I-beam at time of maximum temperature differential. Comparison between theory and experiment.

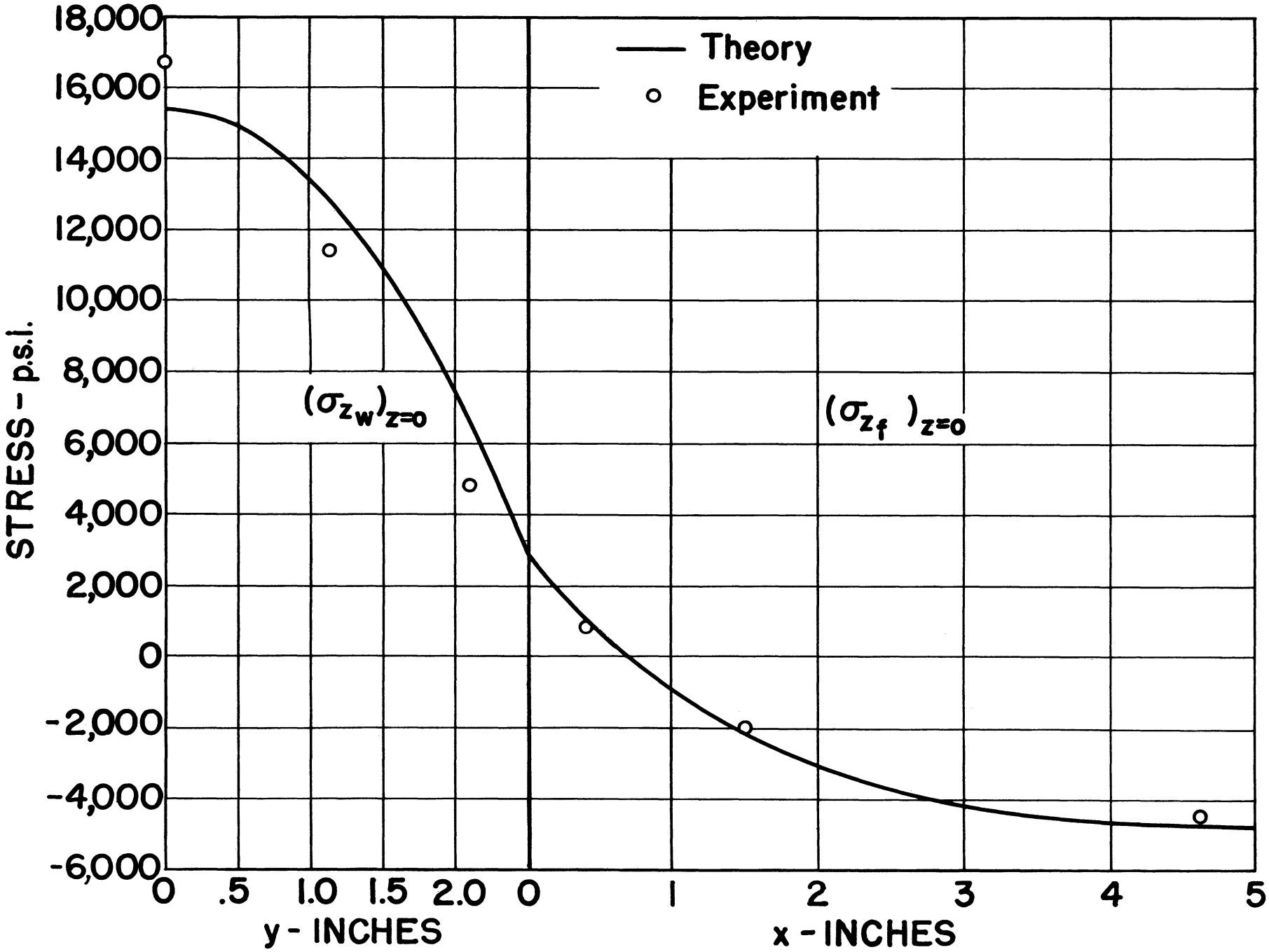

Fig. 27 - Distribution of logitudinal stress in middle section of I-beam at time of maximum temperature differential.

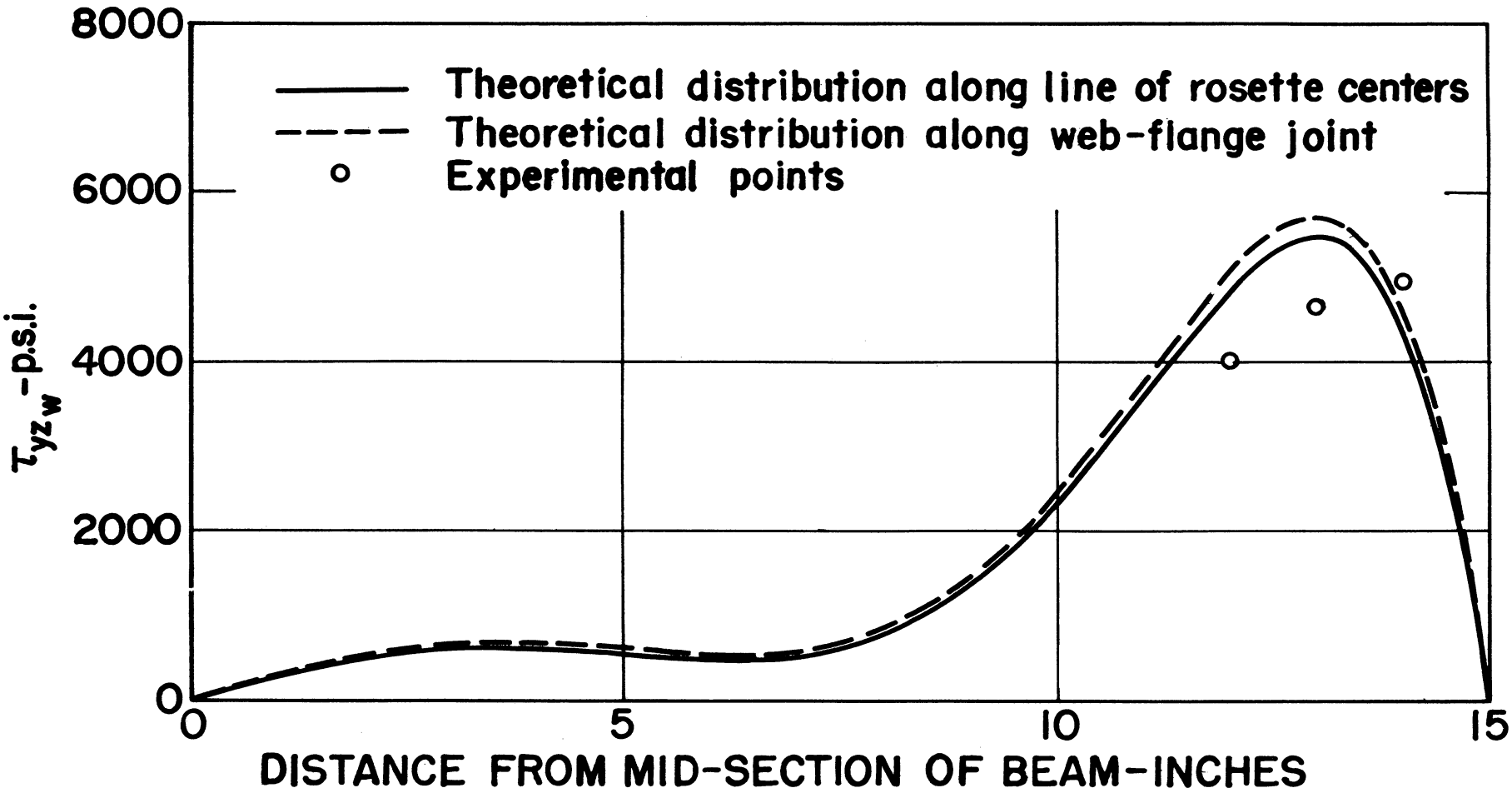

Fig. 28 - Distribution of shear stress in web of I-beam at time of maximum temperature differential. Comparison between theory and experiment.

REFERENCES

1. Johnson, H. A., and Rubesin, M. W., Aerodynamic Heating and Convective Heat Transfer - Summary of Literature Survey, Trans. A. S. M. E., Vol. 71, No. 5, July, 1949, pp. 447-456.

2. Jakob, M., Heat Transfer, Vol. I, John Wiley and Sons, New York, 1949.

3. Austin, J. B., The Flow of Heat in Metals, U. S. Steel Corporation, Research Labs., Kearney, N. J., Series of Lectures Presented to A. S. M. 23rd National Metal Congress and Exposition, Philadelphia, October 20-25, 1941.

4. Carslaw, H. S., and Jaeger, J. C., Conduction of Heat in Solids, Oxford, 1947.

5. Hoff, N. G., Structural Problems of Future Aircraft, Proceedings of Third Anglo-American Aeronautical Conference, Brighton, England, September, 1951.

6. Pohle, F. V., and Oliver, H., Temperature Distribution and Thermal Stresses in a Model of a Supersonic Wing, Jour. Aero. Sciences, Vol. 21, No. 1, January, 1954, p. 8.

7. Timoshenko, S., Theory of Elasticity, First Edition, McGraw-Hill, New York, 1940.

8. Dusinberre, G. M., Numerical Analysis of Heat Flow, McGraw-Hill, New York, 1949.

9. Boole, G., A Treatise on the Calculus of Finite Differences, Third Edition, MacMillan and Company, London, 1880.

10. Isakson, G., A Study of Thermal Stresses in Aircraft Structures Due to Aerodynamic Heating, Doctoral Thesis, Massachusetts Institute of Technology, June, 1953.